

A Study of the Effect of Varying Air-Inflated Seat Cushion Parameters on Seating Comfort

by

Akua B. Ofori-Boateng

Thesis submitted to the Faculty of the
Virginia Polytechnic Institute and State University
in partial fulfillment of the requirements for the degree of
Master of Science

in

Mechanical Engineering

Approved:

Mehdi Ahmadian, Chairman

Don Leo

Mehrdaad Ghorashi

June 2003
Blacksburg, Virginia

Keywords: Seat Cushion, Air-Inflated Seat Cushion, Seating Comfort, Truck
Seat, Cushion, Air-Inflated, Modeling, Simulation, Ofori-Boateng

A Study of the Effect of Varying Air-Inflated Seat Cushion Parameters on Seating Comfort

by

Akua B. Ofori-Boateng

Mehdi Ahmadian, Chairman

Mechanical Engineering

For many years seat cushions have been investigated for their ability to reduce seating discomfort. The objective of this thesis is to examine air-inflated seat cushions to determine how seating comfort (determined by pressure change rate) is affected by changing various parameters of the cushion. To this end, a mathematical model was built using MatLab[®] and SimuLINK[®] to accurately represent the cushion and its response. Different aspects of the cushion, such as seating area, outlet size, cell height, and material elasticity are varied to determine how they each affect seating comfort. For each parameter three different weights are tested to see how the trends observed per parameter are affected by a person's weight.

The results of this study indicate that by changing the base radius, the cell height, the outlet diameter, and the material elasticity of each cell, it is possible to improve seating comfort, as determined by pressure change rate. The study confirms that comfort levels increase with increasing seated area. The study also shows that although increasing the weight of a person decreases the comfort performance of the cushion, not all the trends observed when the cushion parameters are varied remain the same as the person's weight is changed. The trends observed when the cell height and outlet diameter are varied are not affected by the subject weight but all the other trends changed as the subject weight was changed.

ACKNOWLEDGEMENTS

I would like to express my sincere appreciation to all who variously and collectively helped make this thesis possible. Throughout its writing, I have benefited a great deal from the critical comments and suggestions of people who were generous enough to find time not only to read, but also to offer me direction. To this end, I am particularly grateful to Dr. Mehdi Ahmadian, my supervisor, for his immense help and guidance without which this work would not have been possible. Appreciation also goes to Drs. Brian Vick and Al Wicks, for their invaluable comments and direction and to Dr. Dan Inman for his advice and support.

My sincere appreciation goes to Virginia Tech for giving me the opportunity to be part of an excellent tradition, and to the Mechanical Engineering Department for not only accepting me into your field but for providing funding in the form of teaching assistantships. Thanks!

I further express my heartfelt gratitude to all the special friends and colleagues who listened to my partially articulated ideas, read drafts of earlier chapters, assisted me in mapping out my thesis, as well as offering the encouragement that ultimately carried me through. Special mention must be made of Fernando Gonclaves, Jeong-Hoi Koo, Michael Seigler, Chris Boggs, Mathew Rice, Wisdom Gbedemah and David Somuah. Recognition also goes to the numerous friends who in very diverse and special ways made this journey less stressful and more meaningful, especially Kweku Hayford, Maame Araba Nketsiah, Trell Martin, Ben Poe, Harry Baksmaty and the many others who cannot all be named in person. To you all I say, *me dasi pa paa pa bi* for your love, support, and prayers.

There is no doubt that the moral, spiritual and financial support of my family both in Ghana and the United States greatly helped me sail through the rough times. To Mummy, thanks for your prayers and love. To Daddy, thanks for all the encouragement;

despite how unwell you have been, you still came through for me. To Auntie Nana and the gang in Georgia, thanks for the prayers. To Suzanne and Tom Reisinger, thanks again for not only selflessly opening your home to me, but making me feel very wanted and appreciated each time I stepped in.

Finally, I give glory to God Almighty for protecting and sustaining me throughout this journey. Even when it was lonely, stormy, and dark, you gave me the strength to go on, constantly reminding me that, the darker the night gets, the closer it is to dawn.

Given that this is my work, I am, however, solely responsible for any errors or omissions that may be found in this thesis. It merely reflects my mortal limitations.

Akua Boabema Ofori-Boateng
Blacksburg, VA, June 2003

CONTENTS

Abstract	ii
Acknowledgements	iii
List of Figures	vii
List of Tables	x
1 INTRODUCTION	1
1.1 MOTIVATION	1
1.2 OBJECTIVES	3
1.3 APPROACH	4
1.4 OUTLINE	4
1.5 CONTRIBUTION	5
2 BACKGROUND	6
2.1 SEATING DISCOMFORT	6
2.2 DISCOMFORT DUE TO VIBRATION	7
2.3 PRESSURE DISTRIBUTION	9
2.3.1 <i>Pressure Discomfort</i>	11
2.3.2 <i>Quantification of Discomfort</i>	12
2.4 SUMMARY	13
3 MATHEMATICAL MODEL	15
3.1 THE ROHO GROUP'S AIR-INFLATED SEAT CUSHION	15
3.2 RESERVOIR AIR SPRING SYSTEM	16
3.2.1 <i>Flow Rate</i>	22
4 NUMERICAL MODEL	26
4.1 MAIN PROGRAM	26
4.1.1 <i>Initial and Final Conditions</i>	29
4.1.2 <i>Calculating the Mass Flow Rate</i>	30
4.2 MODEL VALIDATION	31

5	RESULTS	38
5.1	VARIABLE PARAMETERS	38
5.2	SEATED AREA	39
5.2.1	<i>Number of Cells in Seated Area</i>	39
5.2.2	<i>Cell Radius</i>	40
5.3	CELL HEIGHT	43
5.4	TOTAL OUTLET AREA	45
5.4.1	<i>Number of Outlets</i>	45
5.4.2	<i>Outlet Diameter</i>	46
5.5	CUSHION MATERIAL PROPERTIES	49
5.5.1	<i>Elasticity</i>	49
5.6	SUBJECT WEIGHT	50
5.7	SUBJECT WEIGHT VERSUS SEATED AREA	51
5.7.1	<i>Subject Weight versus Number of Cells in Seated Area</i>	52
5.7.2	<i>Subject weight Versus Cell Radius</i>	53
5.8	SUBJECT WEIGHT VERSUS CELL HEIGHT	54
5.9	SUBJECT WEIGHT VERSUS OUTLET AREA	55
5.9.1	<i>Subject weight Versus Number of Outlets</i>	55
5.9.2	<i>Subject weight Versus Outlet Diameter</i>	57
5.10	SUBJECT WEIGHT VERSUS MATERIAL ELASTICITY	58
6	CONCLUSION AND RECOMMENDATIONS	60
	References	63
	Appendix A	66
	Vita	69

LIST OF FIGURES

<i>Figure 2.1 Subjective Ratings of Total Discomfort by Time Period for the Four Experimental Conditions. Data are Means for all Subjects on a 0-10 Point Scale where 0 – No Discomfort and 10 - Unbearable. [16].</i>	9
<i>Figure 2.2 Forces acting on a seated operator [18]</i>	10
<i>Figure 2.3 Pressure Distribution Showing Peak Pressures at (a) Ischiatic Tuberosities and (b) Great Trochanters [15].</i>	11
<i>Figure 2.4 Maximum pressures for 10 subjects. Comparison Between Air-Based Seat and Foam Seat. Reprinted from [5]</i>	12
<i>Figure 3.1 An Air-Inflated Seat Cushion. [23]</i>	15
<i>Figure 3.2 Young’s Modulus for Neoprene. Reprinted from [24]</i>	16
<i>Figure 3.3 Simple Representation of Two Air Cells in an Air-Inflated Seat Cushion</i>	17
<i>Figure 3.4 Sum of Forces acting on a Single Cell with no Outlets</i>	22
<i>Figure 3.5 (a) Flow in a Cylindrical Tube using Cylindrical Coordinates and (b) The Axial Velocity Profile.</i>	22
<i>Figure 4.1 Main Program in SimuLINK®</i>	28
<i>Figure 4.2 SimuLINK® Sub-Program for determining the Final Conditions</i>	30
<i>Figure 4.3 SimuLINK® Sub-Program for determining the Mass Flow Rate</i>	31
<i>Figure 4.4 Baseline Case showing Pressure Change and Pressure Change Rate for the Cushion; (a) Pressure Change in seated Area; (b) Pressure Change Rate in Seated Area; (c) Pressure Change in Connected Area; (d) Pressure Change Rate in Connected Area</i>	33
<i>Figure 4.5 Case 1 showing Pressure Change and Pressure Change rate for the Cushion with 100 lb Subject; (a) Pressure Change in seated Area; (b) Pressure Change Rate in Seated Area; (c) Pressure Change in Connected Area; (d) Pressure Change Rate in Connected Area</i>	34
<i>Figure 4.6 Case 2 showing Pressure Change and Pressure Change rate for the Cushion with an Outlet Diameter of 1 inch; (a) Pressure Change in seated Area; (b)</i>	

<i>Pressure Change Rate in Seated Area; (c) Pressure Change in Connected Area; (d) Pressure Change Rate in Connected Area</i>	35
<i>Figure 4.7 Case 3 showing Pressure Change and Pressure Change rate for the Cushion with an Outlet Diameter of Zero; (a) Pressure Change in seated Area; (b) Pressure Change Rate in Seated Area; (c) Pressure Change in Connected Area; (d) Pressure Change Rate in Connected Area</i>	36
<i>Figure 4.8 Case 4 showing Pressure Change and Pressure Change rate for the Cushion with a Cell Number of 12; (a) Pressure Change in seated Cells; (b) Pressure Change Rate in Seated Cells; (c) Pressure Change in Connected Cells; (d) Pressure Change Rate in Connected Cells</i>	37
<i>Figure 5.1 Effect of Number of Cells in Seated Area on the Pcrms Value</i>	40
<i>Figure 5.2 Effect of Base Radius of each Cell on the Pcrms Value</i>	41
<i>Figure 5.3 A Comparison of the Effect of Changing the Seated Area by Increasing the Number of Cells as Opposed to Increasing the Base Area of each cell.</i>	42
<i>Figure 5.4 Effect of Cell Height on Pcrms value</i>	43
<i>Figure 5.5 A Comparison of how each of the Following; Cell Number, Cell Radius and Cell Height Affect Seat Cushion Comfort Performance in Terms of Volume</i>	44
<i>Figure 5.6 Effect of Number of Cell Outlets on the Pcrms Value</i>	46
<i>Figure 5.7 Effect of Outlet Diameter on the Pcrms Value</i>	47
<i>Figure 5.8 A Comparison of how each of the Following; Outlet Number and Outlet Diameter Affect Seat Cushion Comfort Performance in Outlet Area</i>	48
<i>Figure 5.9 Effect of Material Elasticity on the Pcrms Value</i>	49
<i>Figure 5.10 Effect of Internal Pressure on the Pcrms Value</i>	51
<i>Figure 5.11 A Comparison of the Effects of Different Driver Weights on the Pcrms Value by Varying the Number of Cells in the Seated Area</i>	52
<i>Figure 5.12 A Comparison of the Effects of Different Driver Weights on the Pcrms Value by Varying Seated Area in Terms of the Cell Radius</i>	53
<i>Figure 5.13 A Comparison of the Effects of Different Driver Weights on the Pcrms Value by Varying the Cell Height</i>	55
<i>Figure 5.14 A Comparison of the Effects of Different Subject Weights on the Pcrms value by Varying the Number of Outlets per Cell</i>	56

Figure 5.15 A Comparison of the Effects of the Different Subject Weights on the Pcrms value by Varying the Outlet Diameter _____ 57

Figure 5.16 A Comparison of the Effects of Different Driver Weights on the Pcrms value by Varying the Material Elasticity _____ 59

LIST OF TABLES

<i>Table 2.1 Causes of Seating Discomfort [13]</i>	6
<i>Table 2.2 Modified Borg Scale [9]</i>	7
<i>Table 3.1 Table of Variables shown in Figure 3-3</i>	17
<i>Table 4.1 Table of Constants</i>	27
<i>Table 4.2 Variables Used to Validate the Model</i>	32
<i>Table 5.1 Measured Parameters from an Air-Inflated Seat Cushion</i>	38
<i>Table 5.2 % Increase in Pcrms Value per given Increase in Cell Radius</i>	41
<i>Table 5.3 % Increase in Pcrms Value per given Increase in Cell Height</i>	43
<i>Table 5.4 Comparison of the % Decrease in Pcrms Value by Varying the Cell Radius, Cell Number and Cell Height</i>	45
<i>Table 5.5 % Increase in Pcrms Value per Given Increase in Outlet Diameter</i>	47
<i>Table 5.6 A Comparison of the Decrease in Pcrms Value per Driver over the Same Change in Cell Number</i>	53
<i>Table 5.7 A comparison of the Decrease in Pcrms Value per Driver over the Same Change in Cell Radius</i>	54
<i>Table 5.8 A comparison of the Increase in Pcrms Value per Driver over the Same Change in Cell Height</i>	54
<i>Table 5.9 A comparison of the Increase in Pcrms Value per Driver over the Same Change in the Outlet number</i>	56
<i>Table 5.10 A comparison of the Increase in Pcrms Value per Driver over the Same Change in Outlet Diameter</i>	58
<i>Table 5.11 A comparison of the Overall Decrease in Pcrms Value per Subject over the Same Change in Material Elasticity</i>	58

1 Introduction

This chapter begins by explaining the motivation behind the work that is done for this thesis. The objectives and the approach of study are covered and finally an overview that summarizes the thesis and discusses what further study can be done.

1.1 Motivation

Seating comfort is a major concern for drivers and other members of the work force who are exposed to extended periods of sitting and its associated side effects. More than four million truck drivers are engaged in interstate commerce as a result of the widespread dependence on surface transportation of shipping general freight and commodities in the United States [1]. Although there are several other people such as patients who are concerned with seating comfort, drivers represent a large percentage. Research has shown that some of the main factors that affect seating comfort are seat-interface pressure distribution, whole-body vibration and pressure change rate.

Research on the effects of pressure distribution have shown that compression, shear pressures, or both, that develop at the human-seat interface are the main causes of seating discomfort [2, 3]. Based on physics, it is clear that the amount of pressure is proportional to the weight transferred at each point of contact between the body and the cushion. When pressure distribution is uneven then certain parts of the body are exposed to excessive pressures and this can result in pressure ulcers. Pressure ulcers can range from a simple rash to a region of tissue necrosis extending to the underlying bone [4]. The increased pressure on the blood vessels causes decreased blood supply and can result in hypoxia of local tissues, whereas occluded lymphatic drainage can cause damage in deeper tissues [4]. As a result of the research done on this topic it has been found that:

1. Pressures lower than 20 to 30 mmHg are required to prevent capillary occlusion and pressure discomfort due to prolonged sitting [5].

2. Air-filled cushions have been very successful in reducing decubitus ulcers in wheelchair operators by uniformly redistributing pressure across the seat buttocks interface [6].

These findings have led researchers to extend the use of air-inflated seat cushions and consider using them to reduce the whole-body vibration transmitted to seated vehicle operators. Whole-body vibration mainly is applied in the vertical direction to the commercial vehicle operator. Studies of the mechanical response of the seated person to vibration applied in the vertical direction have shown that maximum biodynamic strain is associated with trunk resonance occurring at about 4-8 Hz [7]. Research done by Huston, et al., showed that air-inflated seat cushions were able to reduce vibration transmitted to the seated subjects only for certain subjects at certain frequencies. These findings indicate that if the air-inflated seat cushions are modified in terms of air pressure, shape, and air duct size that it is possible to fine-tune each cushion to reduce the vibration transmitted for all subjects. The way in which each of these factors affects seating comfort is dependent on what the person describes as “comfortable”, for this reason it is important to find an index that can be used as a measure of comfort.

Most of the comfort indices used today are based on what the subjects describe as “comfortable”. Research done by Buckle et al. used a 10-point scale with descriptive anchors as follows [8]

- 1 - Comfortable
- 3 - Slightly uncomfortable
- 5 - Uncomfortable
- 7 - Very uncomfortable
- 9 - Unbearable uncomfortable.

This scale was used in relation to pressure to determine what pressures feel most comfortable to the human. Another scale that has been employed is the modified Borg scale [9, 10]. The modified Borg scale has the subjects rate the quality of ride on a scale of 1 to 10. Verbal descriptors are associated with the numbers where 1 is “comfortable” and 10 is “painful” [9]. Researchers at the Daihatsu Motor Company developed a new

human engineering index for ride comfort in transient conditions, which used body pressure change rate over time. The smaller the change in the body pressure is over time, the higher the ride comfort would be [11].

The current research uses a mathematical model to predict the driver comfort based on the index developed by Daihatsu. In order to do this effectively it is important to be able to predict the pressure rate change experienced by the driver. For the predication of the driver body pressure rate change, a valid model of the air-inflated seat cushion is needed. Since experimentation is time consuming and can be expensive, it begs the question as to whether it is possible to derive parameters without experiments, using the knowledge of the air-inflated seat cushions physical behavior to predict the behavior of the cushion. The ambition of this thesis is to answer that question.

1.2 Objectives

The objective of this research is to

- Write a mathematical model for an air-inflated seat cushion that can be used to determine what aspects of the cushion will affect the rate of change of pressure and thus the comfort of the driver.

The principles to be examined are the rate of change of pressure experienced by the driver as a function of

- cushion pressure (driver's weight)
- seated area
- number of air ducts per air cell
- air duct size
- air cell size
- material stiffness

1.3 Approach

The approach used in this research was first to conduct an extensive literature study on work done in the area of seating comfort and the factors affecting it. The next step was to use fundamental physics principles to create a mathematical model that would accurately represent an air-inflated seat cushion.

The literature search revealed several studies done in the past in the area of seating comfort. Based on what was found, we were able to determine what method of comfort evaluation to use once the model is developed. The mathematical model is built using MatLab[®] and SimuLINK[®]. The air-inflated seat cushion is based on the application of the Pascal law, which states that when pressure is applied to an enclosed fluid, that pressure is transmitted undiminished to every point of the fluid and to the walls of the container. Using this principle, the cushion was modeled such that each air cell acts as a spring with stiffness that is dependent on the internal pressure of the cushion. The sidewall expansion of the cells is modeled using Hooke's law, which states that the expansion of an elastic material is directly proportional to the load applied to it. To validate the model, simple parameters for which the effects are intuitive, such as the effect of the weight of the person and the air duct diameter are varied to see their effect on the rate of change of pressure. Once the model is validated, all the other cushion parameters are varied, while keeping all other parameters fixed. Each parameter is examined to determine how it would affect pressure rate change of the driver. For each parameter, the study considers various rider weights in order to more accurately represent what happens in practice. The initial pressure during each run is 40 mmHg which is often a suitable initial pressure for air-inflated seat cushions.

1.4 Outline

The components of this research that were necessary for obtaining the objectives outlined in Section 1.1 are given in the following chapters. Chapter 2 will give a background on the topic of seating comfort. This includes a discussion of how comfort has been defined in relation to seats, and the factors that have been found to affect it. It also examines

what has been done to improve driver comfort. Chapter 3 will show in detail the equations used in the mathematical model. The simulation programming done using MatLab[®] and SimuLINK[®] is presented in chapter 4. In Chapter 5 the results found by using the simulation are presented and analyzed. Finally, chapter 6 concludes the research based on the results obtained and makes recommendations on further research in this area.

1.5 Contribution

This research adds to previous research done on seating comfort by

1. Providing a tool that can be used to study the effect of different parameters on system comfort performance.
2. Giving information on how air-inflated seat cushions can be modified to suit multiple subjects.
3. Laying a foundation for a larger investigation into the causes and preventions of seating discomfort.

2 Background

The purpose of this chapter is to provide the background for the research conducted in this thesis. This section deals with comfort and the factors that contribute to human seating discomfort, but in particular it looks at comfort in relation to pressure. It also examines what efforts have been made to use air-inflated seat cushions to increase seating comfort.

2.1 Seating Discomfort

Seating discomfort has been examined from a number of different perspectives. The problem with evaluating comfort in regards to pressure or any other factor is that, comfort is very subjective and not easily quantified. By dictionary definition, comfort is “the provision of support and assistance”. Seating discomfort varies from subject to subject and depends on the task at hand. This thesis focuses on truck drivers. Their job requires sitting for long periods of time. The extended period of sitting includes higher risk of back problems, numbness and discomfort in the buttocks due to surface pressure under the thighs [12]. The sources of such discomfort are listed in Table 2.1.

Table 2.1 Causes of Seating Discomfort [13]

Human experience Mode	Biomechanical		Seat/environment
	Physiology causes	Engineering causes	Source
Pain	Circulation occlusion	Pressure	Cushion stiffness
Pain	Ischemia	Pressure	Cushion stiffness
Pain	Nerve occlusion	Pressure	Seat contour
Discomfort	-	Vibration	Vehicle ride
Perspiration	Heat	Material breathability	Vinyl upholstery
Perception	Visual/auditory tactile	Design/vibration	Vehicle cost

Researchers have made efforts toward evaluating and even quantifying comfort in terms of several parameters including vibration transmissibility [14], pressure distribution at the occupant–seat interface [5, 15] and rate of change of human body pressure [11].

2.2 Discomfort due to Vibration

A major portion of the vibration experienced by the occupants of an automobile enters the body through the seat [14]. Whole-body vibrations, which are vertical vibrations, tend to affect the human body the most. These vibrations are transmitted to the buttocks and back of the occupant along the vertebral axis via the base and back of the seat [16]. Since the natural frequency for the human trunk falls in the range of 4-8 Hz, it is expected that the whole-body vibrations that will most largely affect passengers will occur in this frequency range.

Huston, et al. conducted a study to examine how the shape, frequency and amplitude of mechanical shocks affect the comfort response of the seated human. They carried out experiments on 10 subjects (7 males and 3 females) with no history of back pain. The subjects were seated in a truck seat while it was stationary and a set of input signals were used to drive the seat. The signals were designed to be representative of different types of bumps that are encountered while in a vehicle. The subjects rated their level of comfort using the Modified Borg Scale shown in Table 2.2.

Table 2.2 Modified Borg Scale [9]

Modified Borg Scale	
1	Comfortable
2	
3	Slightly uncomfortable
4	
5	Mildly uncomfortable
6	
7	Very uncomfortable
8	
9	Extremely uncomfortable
10	Painful

They found that vibrations at the low frequency of 2 Hz. are even more uncomfortable than at 4, or 6 Hz [9].

Paddan, et al. evaluated the vibration isolation efficiency of seating in 100 commercial vehicles in several categories (cars, vans, lift trucks, lorries, tractors, busses, dumpers, excavators, helicopters, armored vehicles, mobile cranes, grass lollers, and

mowers). The seat isolation efficiency was expressed by the SEAT value, which is defined as

$$SEAT\% = \frac{Vibration\ on\ the\ seat}{Vibration\ on\ the\ floor} \times 100 \quad (2.1)$$

where vibration on the seat and vibration on the floor can be represented by the root mean square (RMS) or vibration dose value (VDV) of the measured signals [14].

Their SEAT values were obtained assuming that each seat could be interchanged between vehicles without altering its transmissibility. Despite this assumption they concluded that, the severity of whole-body vibration exposures in many work environments can be lessened by improvements to seating dynamics [17].

Falou, et al. carried out a study to evaluate indices for fatigue, discomfort and performance of subjects seated for long durations (150 minutes) in a car. They carried out four experiments on 11 male subjects with mean age, height and mass of 35.7 ± 10.4 years, 175.6 ± 5.5 cm, and 75.5 ± 6.1 kg, respectively. The subjects were placed in a car seat on a vibration platform and remained in the seat for the 150 minute duration. The variables measured were Surface electromyography (SEMG) activity, acceleration, subjective discomfort and performance. Their data showed that the subjects rated their discomfort level as increasing with time, as shown in Figure 2.1.

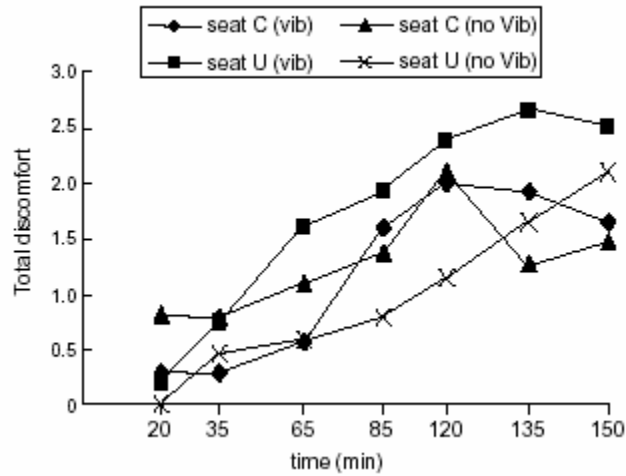


Figure 2.1 Subjective Ratings of Total Discomfort by Time Period for the Four Experimental Conditions. Data are Means for all Subjects on a 0-10 Point Scale where 0 – No Discomfort and 10 - Unbearable. [16].

Hustons, et al. carried out a study using an air-inflated seat cushion built by The ROHO Groups to determine the ability of air-inflated seat cushions to reduce vibrations transmissibility. They found that their cushions were able to reduce vibrations transmitted to the seated subjects only for certain subjects at certain frequencies [6]. They believe that it is possible to fine tune an air-inflated air cushion by varying the air cushion parameters, in order to further attenuate vibration transmissions [6].

The above research indicates that vibration does contribute to discomfort and the longer the subject experiences the vibration, the greater the discomfort could be. It also shows that there is no standard way for measuring comfort where it pertains to vibration.

2.3 Pressure Distribution

Comfort can be partly assessed from the study of the pressure distribution at the human-seat interface [5]. In the seated position there are a number of forces acting on the body as shown in Figure 2.2. The red arrows show the main gravitational forces on the body, and the green arrows show how the seat has to deliver its support. The seat has to:

- keep the correct curvature in the spine
- stop the pelvis tilting backwards
- minimize pressure under the coccyx (tail) and buttocks
- manage high pressure under the pelvis (ischial tuberosities)
- limit pressure under the hamstring muscles
- provide good support under the pelvis and feet

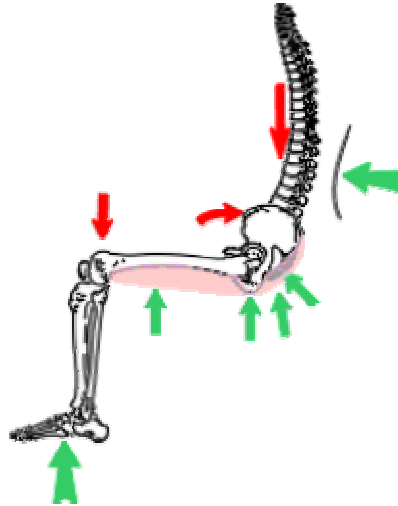


Figure 2.2 Forces acting on a seated operator [18]

A large portion of the support the seat provides comes from the cushion and is concerned with pressure distribution. If the pressure in the seated area is not evenly distributed it can cause areas of high pressure. The areas most commonly affected are those associated with bony prominences, such as the ischial tuberosities and the greater trochanters [19].

Andreoni, et al. carried out a study to determine the interaction between the car driver body with the cushion and the backrest. Their study indicates that the areas, which experience the highest pressure peaks, are the ischiatic tuberosities and the great trochanters, as shown in Figure 2.3.

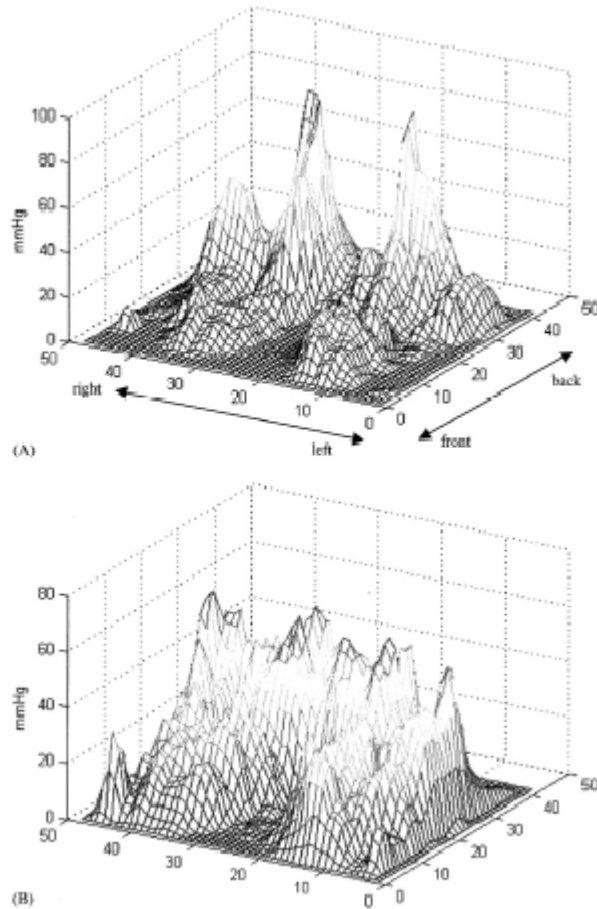


Figure 2.3 Pressure Distribution Showing Peak Pressures at (a) Ischiatic Tuberosities and (b) Great Trochanters [15].

2.3.1 Pressure Discomfort

The generally accepted methods for preventing pressure related discomfort is to reduce duration of high pressure on a particular site by regular repositioning of the sitter or by increasing the distribution through which the pressure is applied for a given time [5].

In examining seating comfort in regards to pressure distribution the first step is to establish a relationship between pressure and comfort. Porter, et al. attempted to do this by investigating the potential value of pressure distribution data for predicting comfort. They recorded interface pressure data for three car seats and what they found was that there in no clear relationship between interface pressure data and reported discomfort [20].

Hostens, et al. carried out a study of the pressure distribution of the human-seat interface to assess comfort. They compared the static back and buttocks support pressures between an air-based seat cushion and foam seats. Figure 2.4 shows their results, which indicate that the air seating system performed better with regards to the static pressure [5].

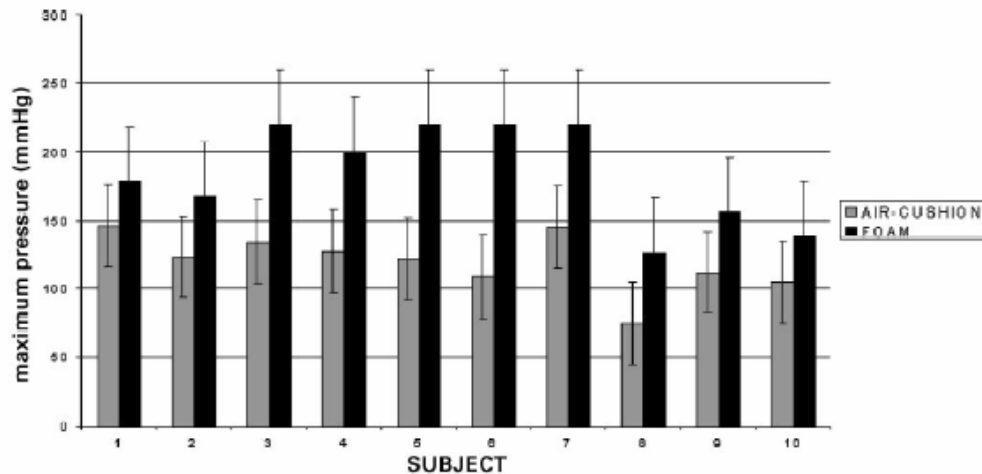


Figure 2.4 Maximum pressures for 10 subjects. Comparison Between Air-Based Seat and Foam Seat. Reprinted from [5]

2.3.2 Quantification of Discomfort

As stated previously, pressure discomfort is qualitative. Several researchers have tried to develop a standard way for measuring discomfort using various techniques.

Shen, et al. carried out an investigation to test the validity of seven existing scales by which discomfort is measured. They tested the following scales

1. Corlett discomfort scale, developed 1976
2. Category partitioning scale developed 1980
3. Borg CR-10 scale, developed 1982
4. Heller scale that rates pain intensity
5. 8-point ordinal scale, developed in 1988
6. Modified intensity and discomfort scale

7. 21-point scale

In their experiment, they placed 12 subjects (6 males, 6 females) in a test-seating device that generated interface pressure from underneath a foam cushion. They set the device to four levels of stimulus, 60, 85, 120, and 165 mmHg. Each subject was then asked to report perceived pressure intensity, discomfort levels due to pressure and overall discomfort using each of the scales they considered. Their findings indicate that the Category Partitioning Scale was the most reliable scale in predicting pressure discomfort.

Other methods for measuring comfort that have been developed more recently are the Pressure Change Rate Root Mean Square (Pcrms) value and the Area Pressure Change Rate Root Mean Square (APcrms) value. These were developed by the Daihatsu Motor Company. Daihatsu researchers showed that the Pcrms value was the most accurate measure for “unpleasant sensation” due to *transient* vibrations [11]. Pcrms is defined as

$$Pcrms = \left[\frac{1}{T} \int_0^T \left(\frac{dP(t)}{dt} \right)^2 dt \right]^{1/2} \quad (2.2)$$

where T is the total time period and P(t) is the dynamic pressure. The research suggests that a lower pressure change rate will result in a more comfortable seat cushion [22].

2.4 Summary

The background information given in this chapter is the foundation upon which the current study is built. Recent research has shown the ability of air-inflated seat cushions to improve pressure distribution, to reduce vibrations transmitted to the driver and to improve overall comfort. The work performed thus far, however, has been limited in showing the full capability of air-seat cushions because of an inability to modify the cushion parameters.

The researchers have all suggested that better results could be recorded for these cushions if it were possible to alter their dimensions to suit each customer. Therefore, the goal of this research is to provide a model that can accurately predict the behavior of

these air cushions and modify the cushion parameters to determine how these modifications affect comfort for multiple users. Our measure of comfort in this study will be the Perms value, which describes user comfort in terms of pressure change rate. This research has the ultimate goal of providing manufactures of the air-inflated seat cushions with the tools to determine exactly what seat cushion parameters can most greatly affect user comfort.

3 Mathematical Model

This chapter introduces the physical characteristics of air-inflated cushions that are commonly used for heavy truck applications. The chapter also discusses the mathematics and physical principles of the seat cushion and the manner by which they are used to create a model that can predict the dynamic behavior of the cushion.

3.1 The ROHO Group's Air-Inflated Seat Cushion

The seat cushion modeled in this study is an air-inflated seat cushion made by The ROHO Groups. The cushion as shown in Figure 3.1 has dimensions of 19 inches by 19 inches and has a cell height of 2 inches when fully inflated. Due to the required immersion of the driver in the cushion, it will raise the driver about 0.5 inches above the seat, when the driver's weight is fully applied to the top of the cushion.



Figure 3.1 An Air-Inflated Seat Cushion. [23]

The cushion weighs approximately 3 pounds and is commonly made of Neoprene rubber, which has a Young's Modulus of approximately 0.8 KPa, as is illustrated in Figure 3.2.

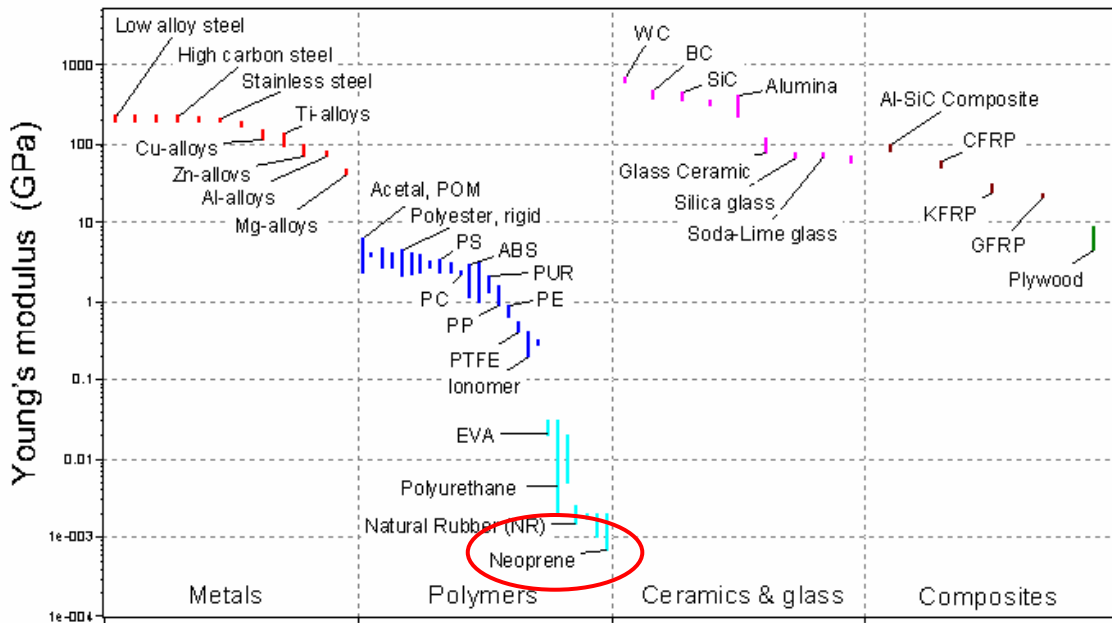


Figure 3.2 Young's Modulus for Neoprene. Reprinted from [24]

The cushion includes interconnected air cells to allow for airflow between the cells. The interconnections allow for the cushion to take the seated profile of the driver which is non-uniform and changes as the driver moves on the seat. The cells act as shock absorbers with damping characteristics dependent on the cell pressure, cell size, and air transfer rate between the cells [23].

3.2 Reservoir Air Spring System

The behavior of the cushion can be modeled in a simplified form by first modeling the behavior of any two enclosures (cells) with compliant walls that are interconnected by a passageway, as is shown schematically in Figure 3.3

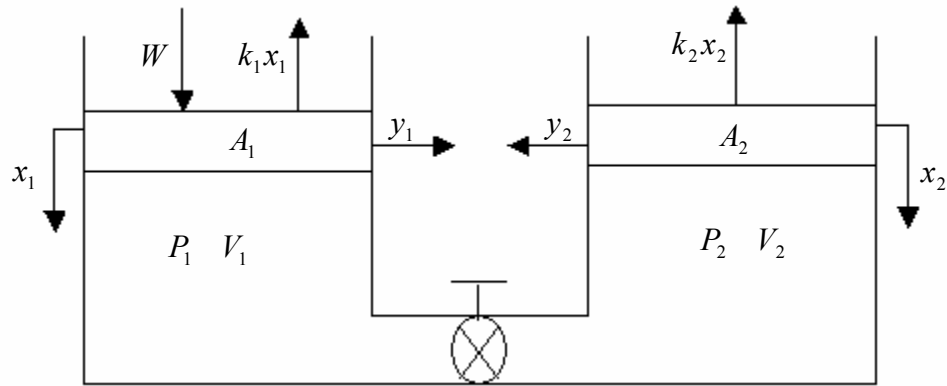


Figure 3.3 Simple Representation of Two Air Cells in an Air-Inflated Seat Cushion

Figure 3.3 employs the use of symbols to simplify the schematic; these symbols are explained in Table 3.1.

Table 3.1 Table of Variables shown in Figure 3-3

Symbol	Description	Units
W	Seated Wight of the person	<i>in</i>
x_1	Vertical compression of cells in seated area	<i>lb</i>
k_1	Stiffness of air in seated area	<i>lb/in</i>
A_1	Seated area	<i>in²</i>
P_1	Pressure in seated area	<i>mmHg</i>
V_1	Volume of air in cells in the seated area	<i>in³</i>
y_1	Horizontal expansion of cells in the seated are due to material elasticity	<i>in</i>
x_2	Vertical compression of cells in unseated area	<i>in</i>
k_2	Stiffness of air in unseated area	<i>lb/in</i>
A_2	Unseated area	<i>in²</i>
P_2	Pressure in unseated area	<i>mmHg</i>
V_2	Volume of air in cells in the unseated area	<i>in³</i>
y_2	Horizontal expansion of cells in the unseated are due to material elasticity	<i>in</i>

This model makes use of the following assumptions:

- The system is isothermal - there is no change in temperature when the air moves from one part of the cushion to another and there is no transfer of heat from the driver's body to the cushion.
- Total mass remains constant - although there is a movement of air from one part of the cushion to another, the total mass of the system remains constant.
- No inter-cell resistance or air dynamics i.e., $P_1 = P_2$ - When equilibrium is reached, the pressure in the seated part of the cushion is equal to the pressure in the connected part.
- Cell compliance acts as linear spring - The amount by which the seated area compresses is directly proportional to the subject weight
- At equilibrium when $W = 0$, $x_1 = x_2 = 0$, $\Delta A_1 = \Delta A_2 = 0$ - when no one is sitting on the cushion, there is no initial compression or expansion of the cells.
- Constant air density - The cushion at 40 mmHg is not turgid, and the cushion is elastic. For these reasons when a weight is applied to the cushion, the change in compression of the air is negligible making it safe to assume constant air density.

Based on these assumptions the conditions at equilibrium i.e., when $W = 0$ and when $W = K$ can be established.

At equilibrium when the driver is completely settled in the cushion, the sum of forces on the seated area gives the equation

$$W - k_1 x_1 = P_1 A_{1_{seated}} \quad (3.1)$$

where W is the seated weight of the driver, k_1 is the stiffness of the cells in the seated area, x_1 is the vertical displacement of the cells in the seated area, P_1 is the pressure in the cells in the seated area, and $A_{1_{seated}}$ is the seated area which is given by the equation

$$A_{1_{seated}} = (A_1 + \Delta A_1) \quad (3.2)$$

where ΔA_1 represents the expansion in the seated area due to the compliance of the material. It should be noted that the seated weight of a person is 80% of their total weight and throughout this study all references made to the weight of the person are referring to full weight of the person and not the seated weight. The seated area is the area over which the seated weight is distributed and refers to the sum of the base areas of each cell in the seated area. This is because each cell is assumed to be a semi-sphere and the resultant pressure due to the force from the driver acts perpendicular to the area of the flat face of the hemisphere and has a magnitude of

$$P_1 = \frac{W}{A_1} \quad (3.3)$$

The compliance of the cells is based on the elastic modulus of the material. The stiffness k of the cells is based on the internal pressure and can be derived by examining a single cell in the seated area with no outlets at the two equilibrium positions. A manipulation of Equation (3.3) shows that

$$F = P_i A_i \quad (3.4)$$

where,

$$A_i = \frac{V_i}{h_i} \quad (3.5)$$

V_i and h_i represent the initial volume and height of the cell respectively. It should be noted that in the transition from Equation (3.3) to Equations (3.4) and (3.5), that P_1 and A_1 changed to P_i and A_i respectively, these represent the initial pressure and area respectively when there is no weight on the cushion. The weight previously represented as W has been changed to F since weight is simply the force a person exerts on a body due to its mass. Using the ideal gas law we can say that the product of the initial pressure and the volume ($P_i V_i$) when there is no weight of the cushion is equal to the product of the final pressure and the volume ($P_f V_f$) when a weight has been applied and equilibrium has been reached. This is shown in Equation (3.6)

$$P_i V_i = P_f V_f \quad (3.6)$$

The final volume V_f represents the new volume of the cushion after the driver's weight has settled. It is slightly smaller than the original volume because although the material is elastic and can expand, the compression due to the subject weight is larger. The final volume is given by Equation (3.7).

$$V_f = V_i - \underbrace{\Delta V}_{Ax} \quad (3.7)$$

Plugging Equation (3.7) into Equation (3.6) gives:

$$P_i V_i = P_f V_i - P_f (Ax) \quad (3.8)$$

this can be written as:

$$\left(\frac{P_i V_i - P_f V_i}{h} \right) h = P_f (Ax) \quad (3.9)$$

or as:

$$(P_i A_i - P_f A_i) h = P_f (Ax) \quad (3.10)$$

and this can be manipulated to give:

$$(F_i - F_f) h = P_f (Ax) \quad (3.11)$$

Rearranging Equation (3.10) gives Equation (3.11) which is related to the Hooke's law according to:

$$\frac{F_i - F_f}{x} = \frac{P_f A}{h} \quad (3.12a)$$

and

$$\frac{F_i - F_f}{x} = k \quad (3.13b)$$

Equations (3.12a) and (3.12b) suggest that the cell stiffness is directly proportional to the final pressure within the system and is inversely proportional to the height of the cell. The cell height h , however does not remain constant and decreases as the cell

compression x increases. Therefore the air stiffness is dependent on the final pressure P_f and the final cell height $h - x$. Based on this the cell stiffness can be written as:

$$k = \frac{A_f}{h - x} P_f \quad (3.14)$$

The next step is to examine the sum of forces on the second cell, which represents the cells that do not directly experience the weight of the driver, which we will refer to as the connected cells. Equation 3.14 gives the force balance on the connected cell area as

$$-k_2 x_2 = P_2 A_2 \quad (3.15)$$

Based on the assumption that at equilibrium $P_1 = P_2 = P$, a relationship can be established between the two cells described by.

$$\frac{W - k_1 x_1}{A_{1_{seated}}} = \frac{-k_2 x_2}{A_{2_{seated}}} \quad (3.16)$$

It should be noted that the above mathematical model represents the dynamic forces that occur at the seat. The static forces resulting from the weight of the person are not included above, since they are counter balanced by the increased pressure that occurs in the cells. This phenomenon is shown in Figure 3.4.

Based on Figure 3.4 the total force on the seated cells is given by:

$$F_{in} = \sum F = -(m_{sitter} \cdot g) - (P_{atm} \cdot A_1) - (m_{air} \cdot g) + P_1 A_1 \quad (3.17)$$

Air takes the shape and size of its container and therefore by determining the change in volume for each cell, the change in air mass between cells can be determined since the density is assumed to be constant. In this particular model, the cells are modeled as semi-spheres and therefore the volume of each cell is

$$V_{seated} = \frac{2}{3} \pi (r + \Delta r)^2 (h - x) \quad (3.18)$$

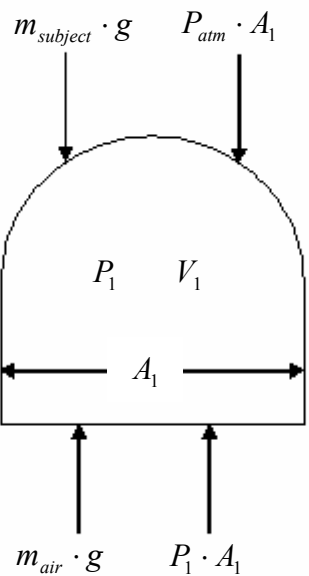


Figure 3.4 Sum of Forces acting on a Single Cell with no Outlets

Knowing the sum of forces acting on the cushion and the sidewall compliance, it is possible to determine the change in cell pressure simply by using the Pascal law. The pressure drop can be used to determine the flow characteristics.

3.2.1 Flow Rate

The flow of air between the cells is laminar and is very similar to the blood flow through animal capillaries. Because of the circular symmetry of the outlets, the air-flow is best described by using cylindrical coordinates, as shown in Figure 3.5 (a).

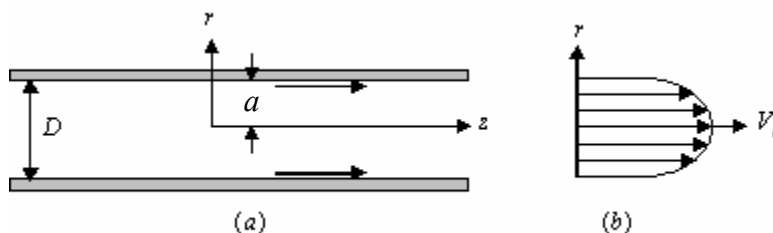


Figure 3.5 (a) Flow in a Cylindrical Tube using Cylindrical Coordinates and (b) The Axial Velocity Profile.

A simplified form of the Navier-Stokes equation for this flow is:

$$\begin{aligned} \frac{d^2 V_z}{dr^2} + \frac{1}{r} \left(r \frac{dV_z}{dr} \right) &= \frac{1}{r} \frac{d}{dr} \left(r \frac{dV_z}{dr} \right) \\ &= \frac{1}{\mu} \frac{dp^*}{dz} \end{aligned} \quad (3.19)$$

where total derivatives have been used because V_z is a function of the radial distance r and p^* is a function of the axial distance z alone. Multiplying Equation (3.19) by r and integrating once gives:

$$r \frac{dV_z}{dr} = \frac{r^2}{2\mu} \frac{dp^*}{dz} + c_1 \quad (3.20)$$

The shear stress in the tube centerline $r = 0$ must be zero because of axial symmetry and thus $dV_z/dr = 0$ at $r = 0$, thereby requiring $c_1 = 0$. Dividing Equation (3.20) by r and integrating gives

$$V_z = \frac{r^2}{4\mu} \frac{dp^*}{dz} + c_2 \quad (3.21)$$

By choosing $c_2 = -a^2 (dp^*/dz)(4\mu)$, the velocity V_z at the wall $r = a$ becomes zero, as it should be at a stationary wall, and the velocity distribution for circular flow is:

$$V_z = \frac{a^2 - r^2}{4\mu} \left(-\frac{dp^*}{dz} \right) \quad (3.22)$$

where a minus sign is multiplying dp^*/dz because the latter is negative for positive V_z , i.e. for flow in the z direction. This velocity distribution is illustrated in Figure 3.5 (b). The volumetric flow rate Q can be found by integrating the axial velocity V_z across the tube cross-section:

$$\begin{aligned}
Q &= \int_0^a V_z (2\pi r) dr \\
&= \frac{r}{2\mu} \left(-\frac{dp^*}{dz} \right) \int_0^a r(a^2 - r^2) dr \\
&= \frac{r}{2\mu} \left(-\frac{dp^*}{dz} \right) \left[\frac{r^2 a^2}{2} - \frac{r^4}{4} \right]_0^a \\
&= \frac{\pi a^4}{8\mu} \left(-\frac{dp^*}{dz} \right) \\
&= \frac{\pi D^4}{128\mu} \left(-\frac{dp^*}{dz} \right)
\end{aligned} \tag{3.23}$$

The volumetric flow rate through a circular tube is very sensitive to the tube diameter D , varying to the fourth power of the diameter. The average flow velocity u_m is obtained by dividing the volumetric flow rate Q by the tube area $\pi D^2/4$:

$$\begin{aligned}
u_m &= \frac{4Q}{\pi D^2} \\
&= \frac{D^2}{32\mu} \left(-\frac{dp^*}{dz} \right)
\end{aligned} \tag{3.24}$$

and the mass flow rate through the tube can be described by:

$$\dot{m} = \rho u_m A_c \tag{3.25}$$

where A_c is the cross-sectional area on the interconnecting tubes.

The relationship between the average flow velocity and the pressure gradient is conventionally expressed in a dimensionless form by defining the Darcy Friction Factor, f as:

$$f \equiv \frac{-(\Delta P/l)D}{\rho u_m^2/2} \tag{3.26}$$

where both the numerator and the denominator of the right hand side of Equation (3.26) have the dimensions of pressure. ΔP is the pressure drop, l is the length of the interconnecting tube, and ρ is the air density. For a circular tube, The Darcy friction factor f can be found by substituting Equation (3.24) into Equation (3.26) giving:

$$f = \frac{64}{\text{Re}_D} \quad (3.27)$$

where Re_D is the Reynolds number.

This chapter has covered the formulation of the mathematical model, which includes the assumptions that were made based on the physical behavior of the cushion. The model examined the force balance on the seated part of the cushion as well as the part of the cushion connected to it. The model also looked at the flow behavior of the cushion and how it can be represented mathematically. The next chapter uses the math and physics explained in this chapter to create the numerical model using MatLab[®] and SimuLINK[®].

4 Numerical Model

This chapter discusses the program used to simulate the cushion behavior when a driver sits on it. The main program and its subroutines are discussed. The chapter also concludes with a description of the ways in which the model is validated.

4.1 Main Program

This chapter discusses the main program as it is designed using MatLab[®] and SimuLINK[®]. The initial cell pressure is assumed to be 40 mmHg which is the recommended pressure for the cushions that we have experimented with at the Advanced Vehicle Dynamics Laboratory. The final cell pressure is determined by the weight of the driver.

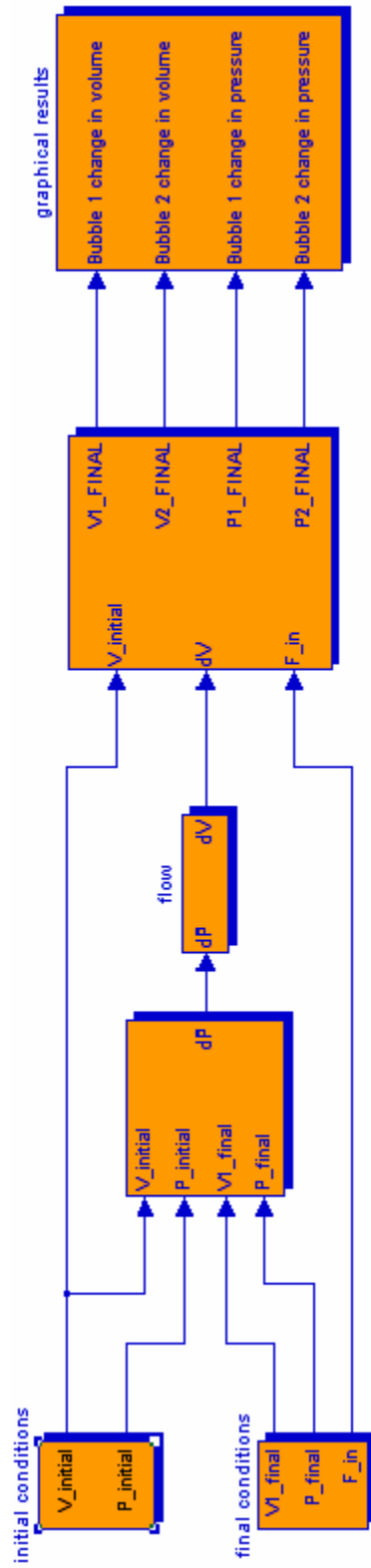
The program first calculates the initial and final conditions based on the defined constants shown in Table 4.1. Without a driver seated on the cushion, the final and initial conditions are exactly the same. When the weight of the driver is applied to the cushion, the program calculates the final cell pressure and volume as well as the differences between the final and initial conditions. This provides the pressure drop that will be used to calculate the volumetric flow rate and as such the air mass flow rate. The change of pressure with time can then be determined from the volumetric flow rate. The program also determines the pressure along with the derivative of pressure plotted versus time for the time it will take for cell pressure to reach equilibrium.

Table 4.1 Table of Constants

Symbol	Description	Value	Units
g	Acceleration due to gravity	32.174	ft/s^2
R	Ideal gas constant	1545	$ft \cdot lbf / lbmol \cdot ^\circ R$
r	Cells radius	1.2	in
h	Cell height	2	in
\bar{P}	Initial equilibrium pressure in system	40	$mmHg$
D	Outlet diameter	0.16	in
l	Outlet length	0.43	in
n_{max}	Maximum number of outlets per cell	4	
N_{max}	Maximum number of cells in seated area	12	
N_{min}	Minimum number of cells in seated area	4	
E	Young's Modulus of material	0.8	KPa
ρ_{air}	Density of air	1×10^{-2}	g/cm^3
P_{atm}	Atmospheric pressure	14.696	lbf/in^2
T_{air}	Air temperature	25 / 77	$^\circ C / ^\circ F$
MM_{air}	Molar mass of air	8×10^{-4}	GPa

Figure 4.1 shows the SimuLINK[®] code for the main program. The main program is broken up into several sub programs which model each of the previously mentioned steps. The next few sections discuss the sub programs that constitute the main program.

Figure 4.1 Main Program in SimuLINK®



4.1.1 Initial and Final Conditions

This section discusses the way the program determines the final and initial conditions. The initial conditions are set by the user, and are incorporated into the program using the MatLab[®] code in Appendix A. The program uses the weight of the seated person to determine the cell stiffness, sidewall expansion, and cell compression as well as the final cell pressure. The cell stiffness, which depends on the air pressure, cell area, cell height and cell compression, is calculated using Equation (3.14). The cell compression x is based on Hooke's law and is determined by the equation

$$W = kx \quad (4.1)$$

The side wall compliance y is determined according to:

$$y = \frac{Wr}{A\varepsilon} \quad (4.2)$$

where W is the seated weight of the driver, r is the base radius of each cell, A is the area of each cell, and ε is the modulus of elasticity. The cell base radius, the seated area, and the cell wall compliance are dependent on each other and continue to change until steady state is reached. Determining these factors make it possible to find the new volume using Equation (3.18) and also to determine the change in pressure using the Pascal law. Figure 4.2 shows the program that determines final conditions of the cell. Once the initial and final conditions are determined, the pressure drop is calculated according to Equation (3.6) and it is used to determine volumetric flow rate Q .

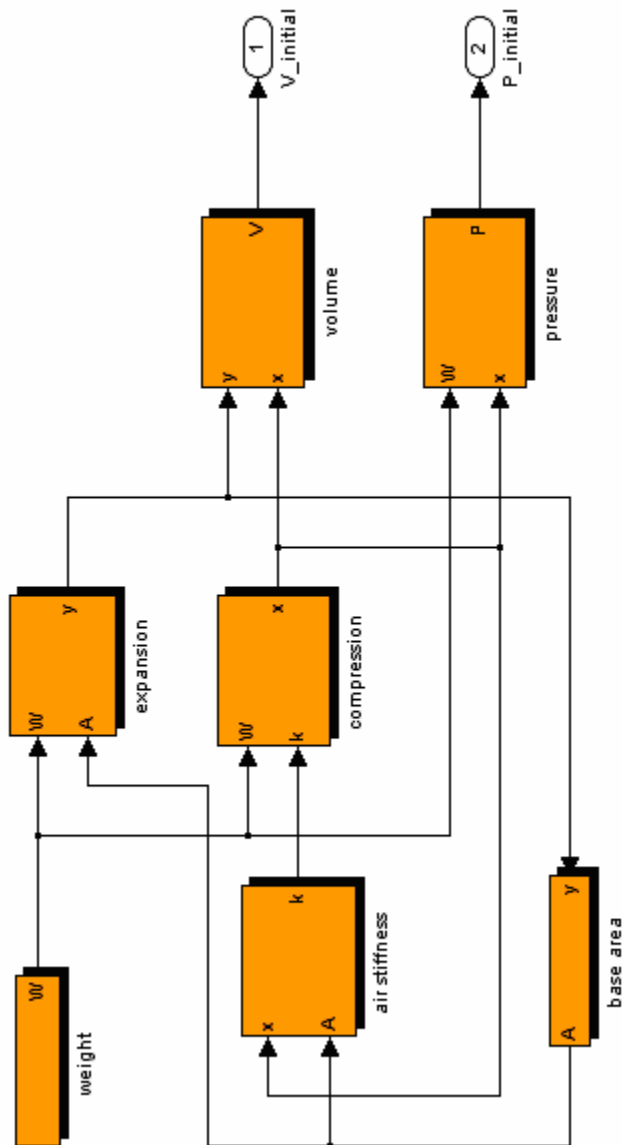


Figure 4.2 SimuLINK[®] Sub-Program for determining the Final Conditions

4.1.2 Calculating the Mass Flow Rate

This section shows the numerical model that is used to determine the mass flow rate, which is based on Equations (3.24), (3.25), (3.26), and (3.27). Figure 4.3 shows the SimuLINK[®] code for determining the mass flow rate.

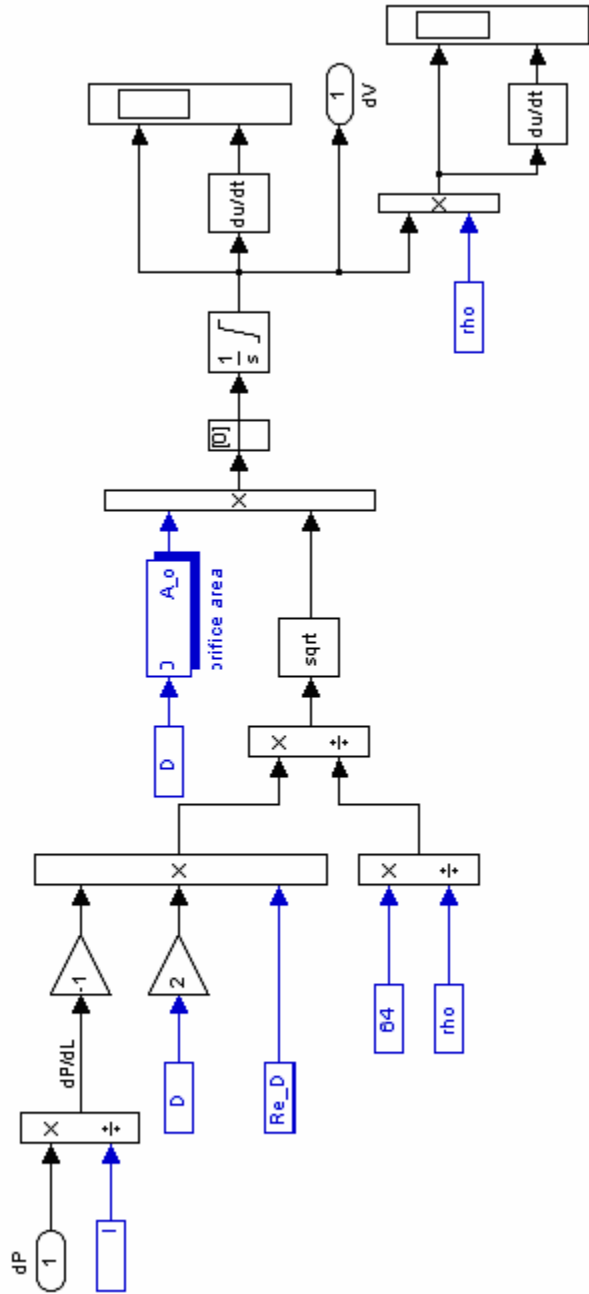


Figure 4.3 SimuLINK[®] Sub-Program for determining the Mass Flow Rate

4.2 Model Validation

This section describes the validation of the model. In order to ensure that the model is functioning properly, it is necessary to check if it responds as expected to particular parameter changes. For instance, it is expected that as the seated weight increases the

final cell pressure will increase; or as the outlet diameter decreases to zero the rate of change of pressure also decreases to zero. It is also expected that there will be a relationship between the cells in the seated area and the connected cells such that the cell pressures should reach equilibrium at the same time. To determine whether these expectations of the model will be fulfilled the parameters shown in Table 4.2 are varied.

Table 4.2 Variables Used to Validate the Model

	weight (lbs)	outlet diameter (in)	Cell Number
Baseline	160	0.16	6
Case 1	100	0.16	6
Case 2	160	1.00	6
Case 3	160	0.00	6
Case 4	160	0.16	12

Figures 4.4, 4.6, 4.7, and 4.8 show the change in pressure over time and the pressure change rate over time for the cells in the seated and connected cell areas for each of the parameters that is varied.

The first case that is examined is what we will call the Baseline case. This case represents a situation in which all parameters are held constant, the driver's weight is 160 pounds, the outlet diameter is 0.16 inch and the number of cells in the seated area is 6. The number of cells in the seated area represents the number of cells over which the driver's seated weight is distributed. It should be noted the time $t = 0$ in the program represents the instant when an input signal (such as a driver would experience due to bumps in the road) is transmitted to the seat, and the time $t = t_{steady\ state}$ is when the driver has settled after responding to that signal. The graphs show the changes that occur in terms of pressure from that instant until equilibrium is reached. Figures 4.4 shows the results obtained for this baseline case. All the other cases are compared to this case to determine the validity of the model.

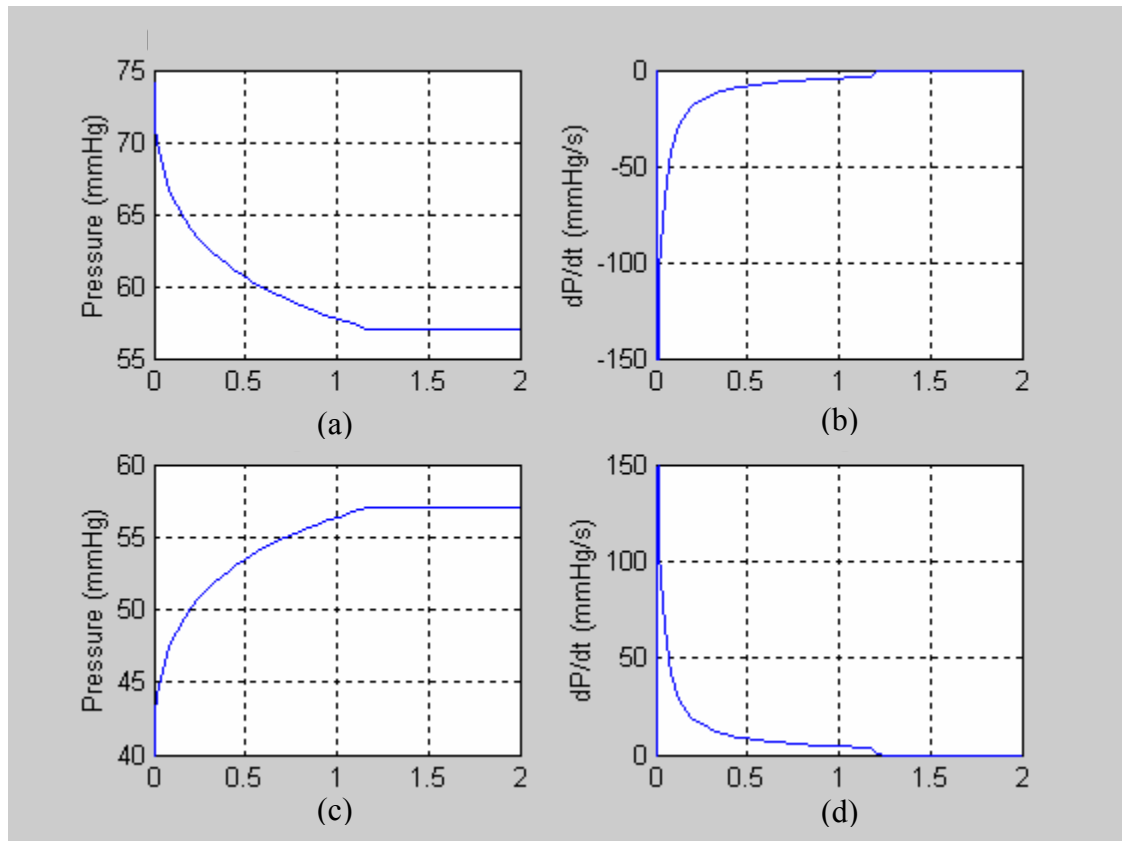


Figure 4.4 Baseline Case showing Pressure Change and Pressure Change Rate for the Cushion; (a) Pressure Change in seated Area; (b) Pressure Change Rate in Seated Area; (c) Pressure Change in Connected Area; (d) Pressure Change Rate in Connected Area

The pressure in the cells in the seated area starts out high due to the input signal. As the air flows out of those cells and the height of cells decrease, the seated area expands thus causing the pressure to decrease. The pressure in the surrounding cells increases at the same rate as the decrease in pressure of the seated area cells, and this continues until equilibrium is reached. As shown in Figure 4.4 the pressure change rate in both cases is exactly the same. This confirms the connection between the cells in that the air flowing out of one cell flows into the next cell at the same rate.

Case 1: In this case we keep all the parameters constant but reduce the weight of the subject to 100 pounds. In this case it is expected that the pressure change and the pressure change rate will be lower than the baseline case. Figure 4.5 which shows the results obtained for this case indicates that decreasing the weight of the driver decreases the final pressure and the pressure change rate.

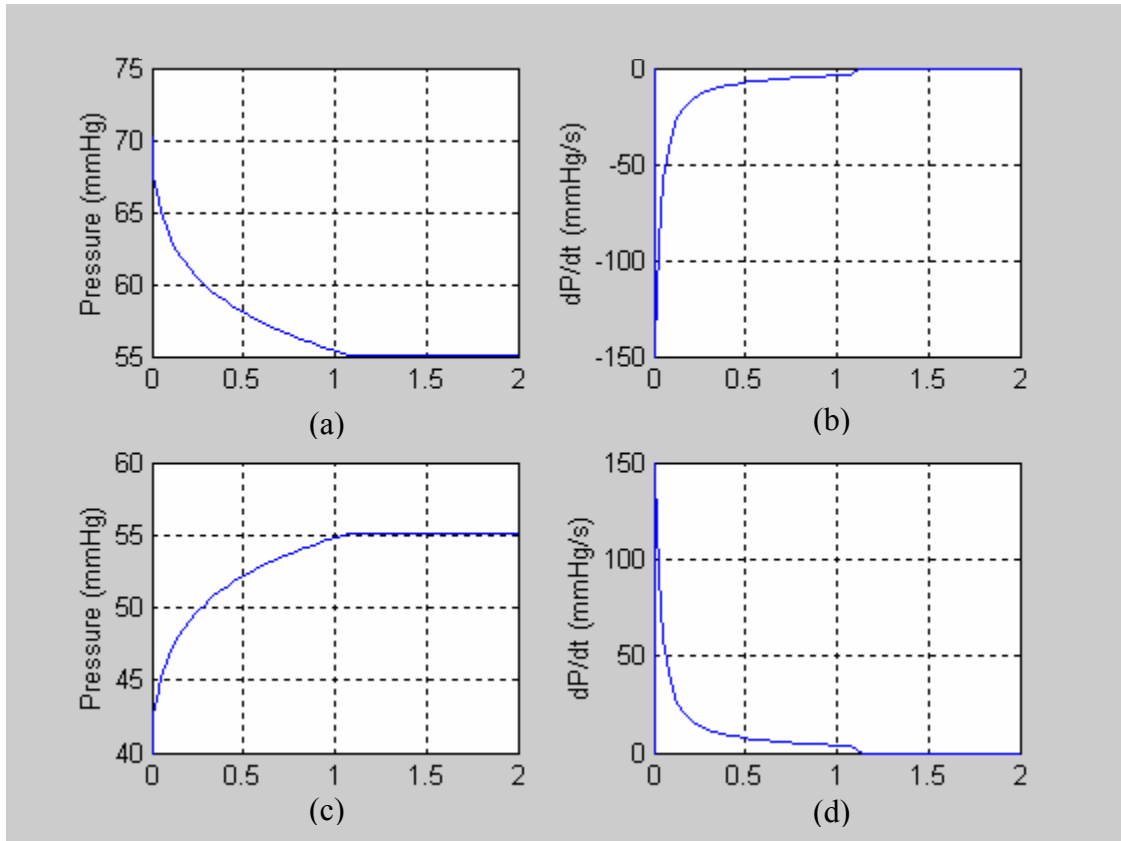


Figure 4.5 Case 1 showing Pressure Change and Pressure Change rate for the Cushion with 100 lb Subject; (a) Pressure Change in seated Area; (b) Pressure Change Rate in Seated Area; (c) Pressure Change in Connected Area; (d) Pressure Change Rate in Connected Area

This validates the fact that the model does not violate the Pascal law. Since the number of cells in the seated area remains constant, it is expected that as the weight is decreased the final pressure will also decrease. The rate of change of pressure change as expected to decrease due to the fact that a lighter weight causes a smaller pressure drop and therefore a lower pressure gradient.

Case 2: Figure 4.6 shows the results obtained for increasing the outlet diameter from 0.16 inch to 1 inch. The driver weight is maintained at 160 Pounds. In this case it is expected that the air will rush through the outlet at an extremely high rate since the outlet area is so large. The final pressure should not change from that of the Baseline case because the driver's weight does not change.

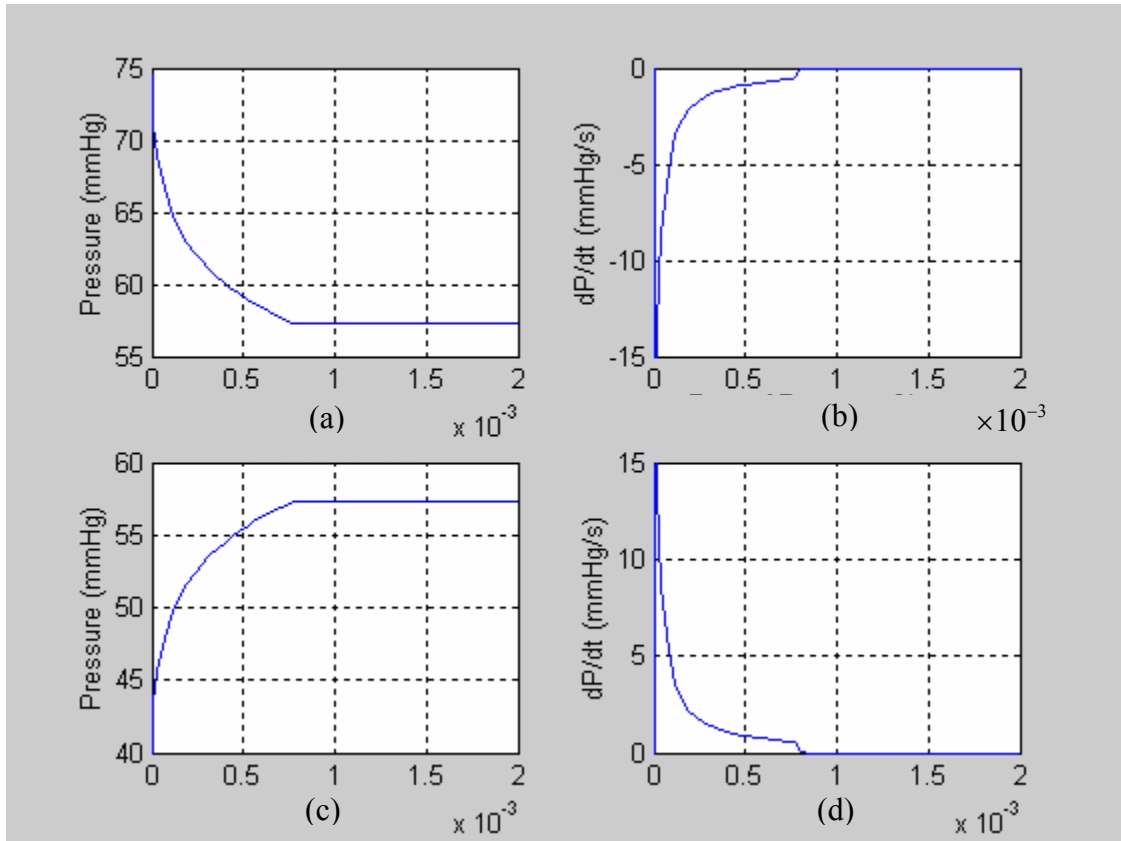


Figure 4.6 Case 2 showing Pressure Change and Pressure Change rate for the Cushion with an Outlet Diameter of 1 inch; (a) Pressure Change in seated Area; (b) Pressure Change Rate in Seated Area; (c) Pressure Change in Connected Area; (d) Pressure Change Rate in Connected Area

The figure shows that the final pressure remains the same as expected and the pressure change rate is so high that equilibrium is achieved almost instantaneously.

Case 3: For this case the outlet diameter is reduced to 0, fully closing the interaction between the seated and connected areas. It is expected that in this case the pressure in the seated area at time $t = 0$ will be at a peak pressure and remain there since there is no relief. In the connected area (which in this case is not actually connected) it is expected that the cell will remain at initial pressure. The pressure change rate in both cases should be zero. Figure 4.7 shows the results that these intuitive observations match with. The rate of change of pressure remains at zero and the peak pressure in the seated area starts at 74.08 mmHg and remains there since there is no relief for it.

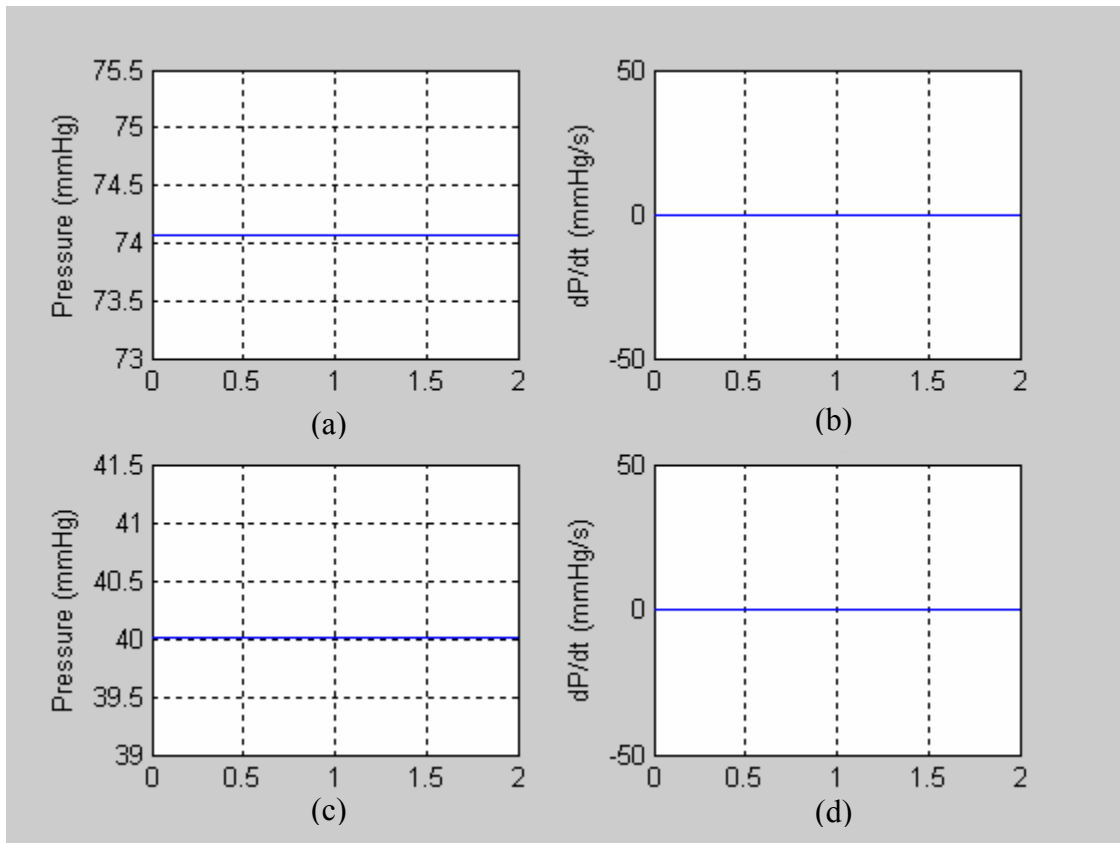


Figure 4.7 Case 3 showing Pressure Change and Pressure Change rate for the Cushion with an Outlet Diameter of Zero; (a) Pressure Change in seated Area; (b) Pressure Change Rate in Seated Area; (c) Pressure Change in Connected Area; (d) Pressure Change Rate in Connected Area

Case 4: In our final case the number of cells in the seated area is increased to 12. It is expected that by increasing the seated area, the final pressure will decrease, and the rate of change of pressure will also decrease. Figure 3.9 shows the response of the cushion to an increase in the seated area. In this case the final pressure is reduced from the Baseline case pressure and so is the rate of change of pressure. Although the rate of change of pressure has reduced the time it takes to reach equilibrium is still short. This is due to the fact that the program evenly divides the weight of the subject over the surface area. So the fact that the surface area is large means that the weight per cell over that area is tantamount to having a light weight person over a smaller area.

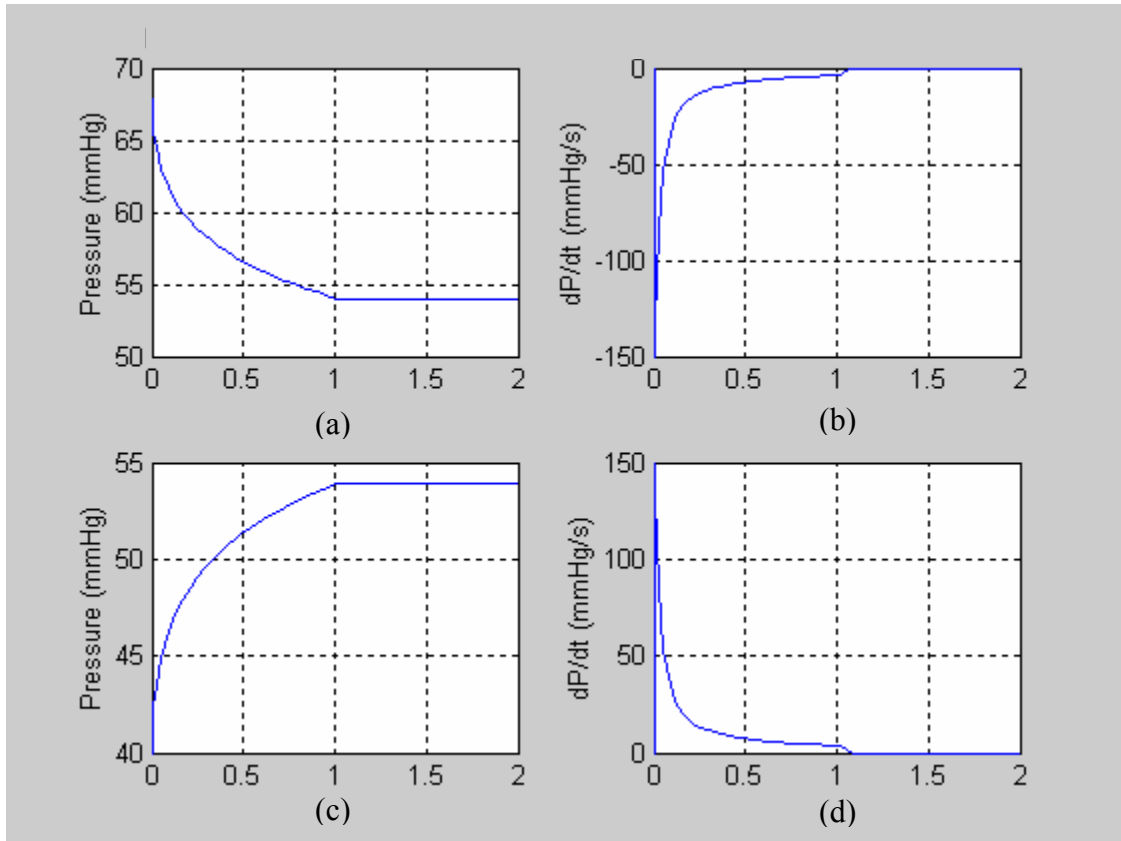


Figure 4.8 Case 4 showing Pressure Change and Pressure Change rate for the Cushion with a Cell Number of 12; (a) Pressure Change in seated Cells; (b) Pressure Change Rate in Seated Cells; (c) Pressure Change in Connected Cells; (d) Pressure Change Rate in Connected Cells

The cases documented above indicate that the program is capable of giving an accurate representation of the behavior of an air-inflated seat cushion. It should be noted that the graphs above have a characteristic kink which would imply that the pressure suddenly hits steady state. This kink is actually just a function of the time step that was used in the programming software. The transition to steady state is quite smooth as long as the time step is small enough. The next chapter will provide the results that are obtained from our parameter studies to evaluate how much each parameter affects the comfort performance of the seat cushion, as measured by Perms.

5 Results

This chapter presents the results that are obtained from our case study. For each case, one parameter is varied while the others are kept constant. The cushion parameters that are examined for their effect on the comfort performance of an air-inflated seat cushion are; the number of cells over which the seated weight is distributed, the cell radius, cell height, the number of outlets per cell, the diameter of each outlet, and the elasticity of the cushion material. Each of the results shown in this section is representative of the effects observed when a person weighing 150 pounds, that is a person with a seated weight of 120 pounds (80% of weight) is placed on the cushion.

This chapter also presents the data that is obtained by reexamining each of the previously mentioned parameters but this time with people of different weight. Although it is known that as the weight of a person increases the pressure and the rate pressure rate change will increase, it is not clear how people of different weights will affect the trends observed in the study. For each of the cases, the P_{crms} value was calculated using Equation (2.2).

5.1 Variable Parameters

A comfort analysis is done on air-inflated seat cushions by varying the parameters seen in Table 5.1. For each parameter, unless the parameter itself is being varied it has a value shown in Table 5.1.

Table 5.1 Measured Parameters from an Air-Inflated Seat Cushion

Symbol	Description	Value	Units
N	Number of cells in seated area	6	
r	Cells radius	1.2	in
h	Cell height	2	in
n	Number of outlets	1	
D	Outlet Diameter	0.16	in
E	Young's Modulus of material	0.8	KPa

The length of each outlet / interconnecting tube is 0.43 inch and initial pressure in all cases remained at 40 mmHg..

5.2 Seated Area

This section examines the relationship between the Pcrms value and the size of the seated area. The size of the area is affected by two parameters, the number of cells that make up the area and the base radius of each cell in the seated area. The first to be examined is the number of cells in the seated area. The dimensions of each cell are kept constant while the number of cells over which the seated weight is distributed is changed. In examining the base radius of each cell, the number of cells in the seated area is kept constant and the radius of each cell is varied. The next two sections examine the effect of changing the seated area on the Pcrms value.

5.2.1 Number of Cells in Seated Area

This section looks at the effect of the changing the seated area by changing the number of cells over which seated weight is distributed. In this case the number of cells is varied from 4 cells to 12 cells. Figure 5.1 shows the results that are obtained.

As the seated area increases, the Pcrms value decreases. This implies that as the seated area increases the higher the comfort performance of the seat cushion. Increasing the number of cells in the seated area by from 4 cells to 12 cells caused a 24% decrease in Pcrms value. The next section considered the other option for increasing the seated area, which is to maintain the number of cells in the seated area and increase the base radius of each cell.

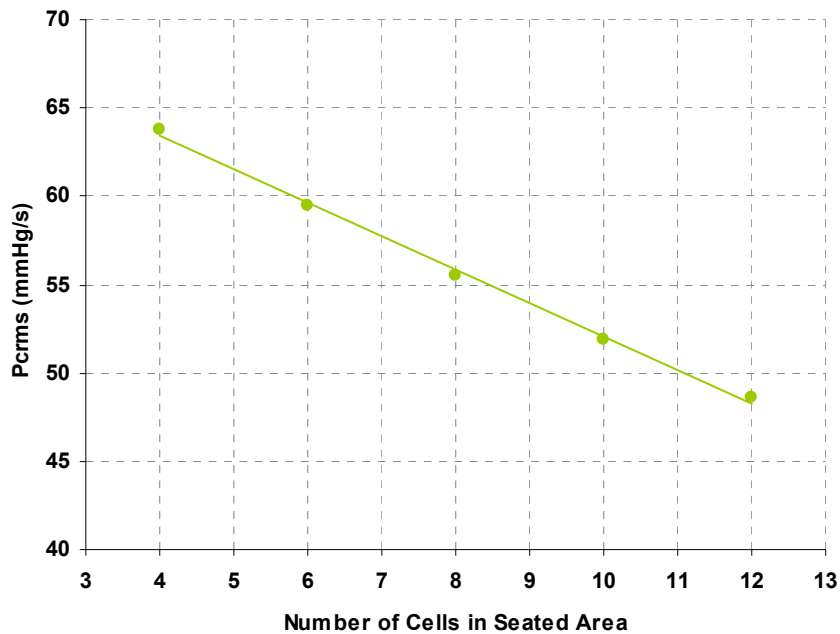


Figure 5.1 Effect of Number of Cells in Seated Area on the Pcrms Value

5.2.2 Cell Radius

This section examines the effect of changing the seated area by changing the base radius of each cell. In this case the number of cells in the seated area remains constant as the base radius of each cell increases. The air-inflated seat cushion used in this study has a cell radius of 1.2 inches. In our study we varied the base radius from 0.8 inch to 1.5 inches. Figure 5.2 shows the results that are obtained.

Increasing the radius from 0.8 inch to 1.5 inch caused a 76% decrease in the Pcrms value. Unlike in the cell number case the decrease is not linear, the gradient begins sharply and as the radius increases the slope of the curve decreases. This indicates that there will come a point where a further increase in cell radius will not have a significant effect on the Pcrms value.

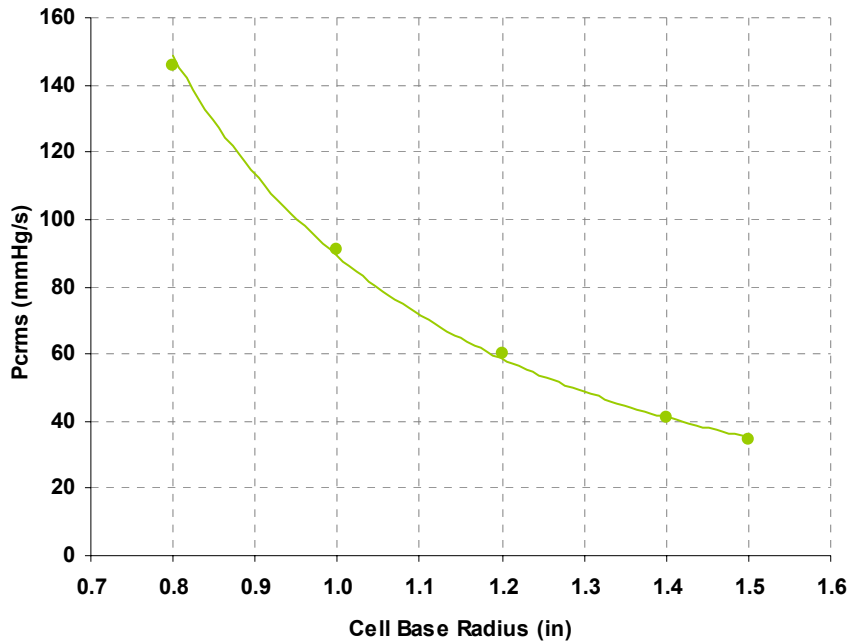


Figure 5.2 Effect of Base Radius of each Cell on the Pcrms Value

Since the relationship is not linear Table 5.2 gives a breakdown of the changes that were observed.

Table 5.2 % Increase in Pcrms Value per given Increase in Cell Radius

Initial radius (in)	Final radius (in)	% change
0.8	1.0	37.63%
1.0	1.2	34.08%
1.2	1.4	31.31%

From Table 5.2 it is clear that as the radius increases the percentage Pcrms value decreases steadily.

Both graphs show that increasing the seated area lowers the Pcrms value and as such increases the comfort performance of the seat cushion. Although the decrease in the Pcrms value is greater for the cell radius case than for a cell number case, no conclusions can be drawn about which method is most effective unless the two methods are compared.

For design purposes it is important to know which method of increasing the seated area gives a better comfort performance. In other words, it is important to

establish whether it better to have a few large cells in the seated area or several small cells in the seated area. Figure 5.3, compares the two methods.

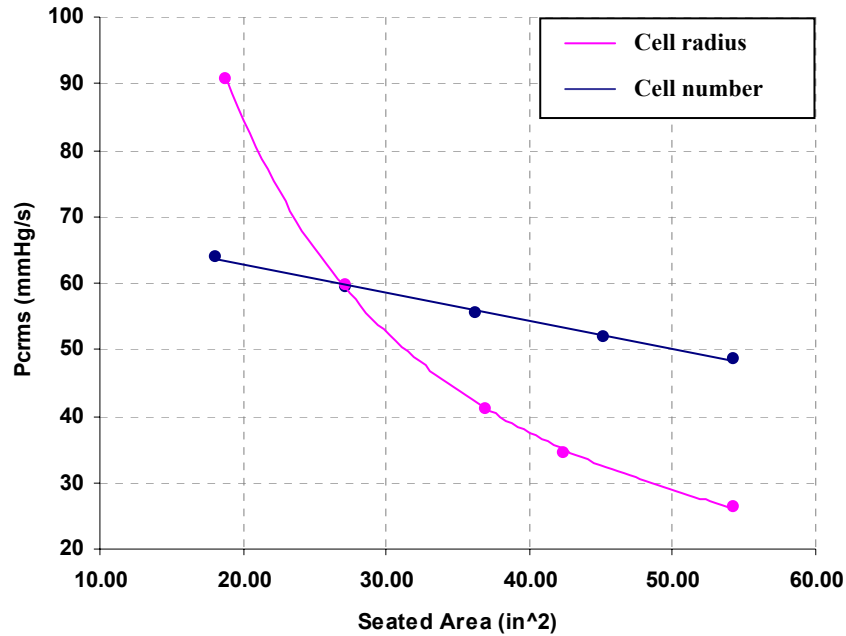


Figure 5.3 A Comparison of the Effect of Changing the Seated Area by Increasing the Number of Cells as Opposed to Increasing the Base Area of each cell.

In each case the seated area is increased from 27 in^2 to 54 in^2 . In the cell number case, this is done by increasing the number of cells from 6 cells to 12 cells and in the cell radius case this is done by increasing the cell radius from 1 inch to 1.5 inches.

This increase in seated area caused an 18% decrease in Pcrms value for the cell number case and a 58% decrease in the Pcrms value for the cell radius case. This suggests that the comfort performance of the cushion is more sensitive to changes in the cell radius than it is to changes the cell number. It should be noted that the graph shows that there is a point with an area of approximately 27 in^2 where the two graphs merge. This point represents the point at which all the parameters have the numerical values shown in Table 5.1. The next parameter to be examined for its effect on comfort performance is the cell height.

5.3 Cell Height

In this case the cell height is varied while keeping all the other parameters constant. The cell height is increased from 1 inch to 4 inches and as is shown in Figure 5.4 this change caused a decrease in the Pcrms value.

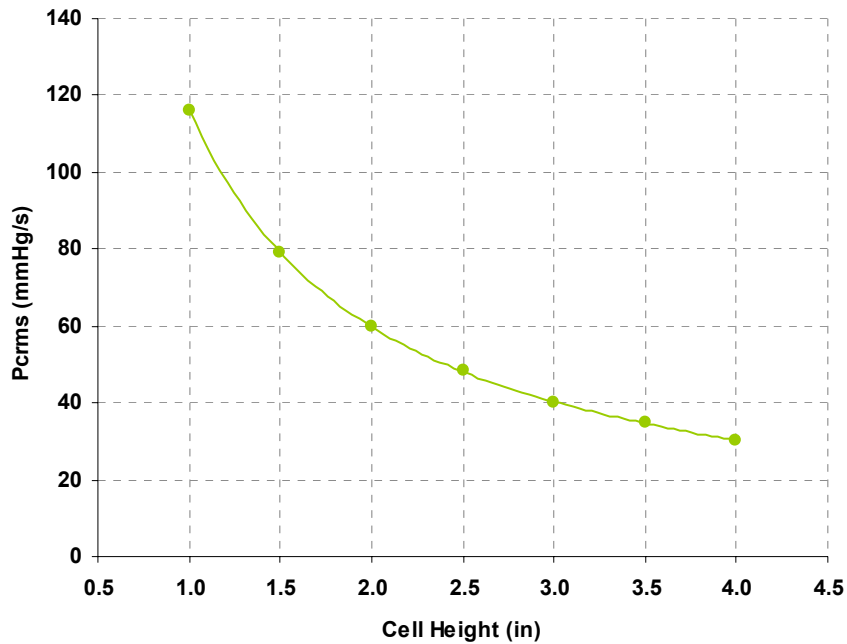


Figure 5.4 Effect of Cell Height on Pcrms value

For this increase in cell height there is a 74% decrease in the Pcrms value. This suggests that the comfort performance of the cushion can be optimized by increasing the cell height; however it is important to pay attention to the fact that increasing the cell height can decrease the pelvis stability of the driver. The relationship between Pcrms value and the cell height is not linear and Table 5.4 shows how the value decreases with increasing cell height.

Table 5.3 % Increase in Pcrms Value per given Increase in Cell Height

Initial height (in)	Final height (in)	pcrms % change
1.0	1.5	32.05%
1.5	2.0	24.30%
2.0	2.5	19.52%
2.5	3.0	16.32%
3.0	3.5	14.04%
3.5	4.0	12.32%

Changing the cell height, cell radius, and the number of cells in the seated area essentially means changing the volume of air that can potentially be displaced by the driver, which we will now refer to as the seated volume. To compare how each of these parameters affects the Pcrms value, a comparison of each of them is done with respect to seated volume. The volume is increased from 36.2 in^3 to 72.4 in^3 . In the case of the cell number this is an increase from 6 cells to 12 cells, in the case of the cell radius this is an increase from 1.2 inches to 1.6 inches, and in the case of the cell height this is an increase from 2 inches to 4 inches

Figure 5.5 shows that in all cases as the seated volume increases the Pcrms value decreases indicating an increase in the comfort performance of the cushion.

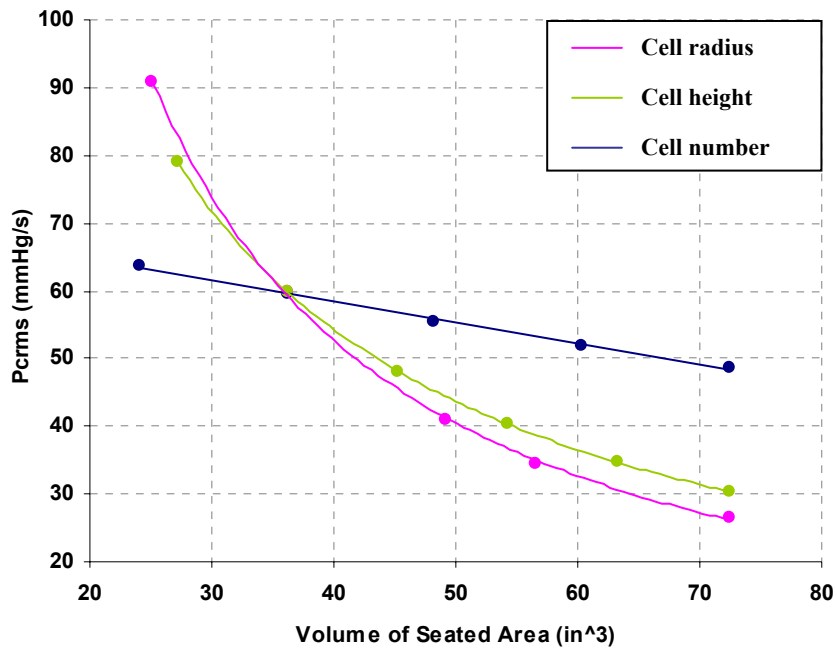


Figure 5.5 A Comparison of how each of the Following; Cell Number, Cell Radius and Cell Height Affect Seat Cushion Comfort Performance in Terms of Volume

The graph shows that increasing the cell radius will lower the Pcrms value the most while increasing the number of cells in the seated area lowers the Pcrms value the least. Table 5.5 shows the percentage decrease per parameter obtained by increasing the volume from 36.2 in^3 to 72.4 in^3 .

Table 5.4 Comparison of the % Decrease in Perms Value by Varying the Cell Radius, Cell Number and Cell Height

Parameter	% Decrease in Perms Value
Cell radius	58%
Cell height	49%
Cell number	18%

The next section discusses the effects the area of the interconnecting outlets has on the comfort performance of an air-inflated cushion.

5.4 Total Outlet Area

Much like resistors in an electrical circuit, the outlets or interconnection between the air cells act to control the flow of air from cell to cell, the smaller the total outlet area of the outlets, the more restricted the air flow and vice versa. There are two ways of varying the outlet area. One way is to control the number of outlets per cell, the other way is to maintain the number of outlets and change the outlet diameter. The next two sections look at the sort of trends that are observed when the outlet area is varied. The first of these to be examined is the number of outlets.

5.4.1 Number of Outlets

The response of the cushion to the number of outlets is intuitive, since it acts to restrict the air flow, the larger the outlet area, the faster the air will flow and the faster the pressure within the system will change. In this part of the experimentation the number of outlets was increased from 0 to 4 outlets per cell. Figure 5.6 shows that this increase in the number of outlets caused a 219 mmHg/s increase in the Perms value.

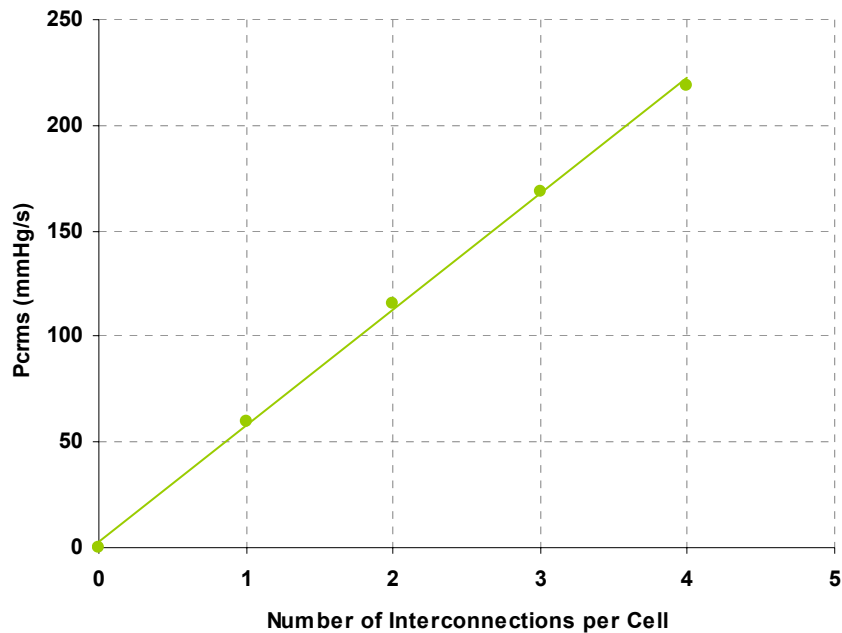


Figure 5.6 Effect of Number of Cell Outlets on the Pcrms Value

The next case study was to examine how keeping the number of outlets constant and varying the outlet diameter would affect the comfort performance.

5.4.2 Outlet Diameter

In this study the outlet diameter is increased from 0 to 0.35 inches. Figure 5.7 shows that this increase in the outlet diameter caused a 332 mmHg/s increase in the Pcrms value. Unlike in the outlet number case the decrease in not linear, the gradient is very shallow at the beginning and as the diameter increases the slope of the curve becomes steeper. This indicates that there will come a point where the outlet will be so large that the flow can no longer be assumed to be laminar and will be approaching turbulent flow. Therefore after a certain point increasing the outlet diameter will not have a significant effect on the Pcrms value.

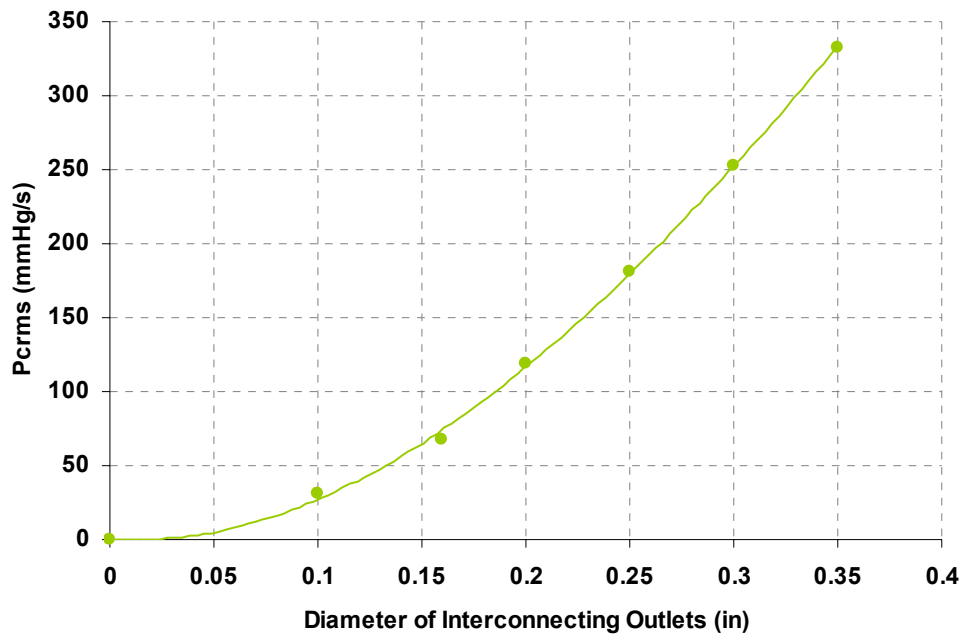


Figure 5.7 Effect of Outlet Diameter on the Pcrms Value

This relationship is not linear and Table 5.5 shows the percentage change over the previous Pcrms value per increase in diameter.

Table 5.5% Increase in Pcrms Value per Given Increase in Outlet Diameter

Initial diameter (in)	Final diameter (in)	pcrms % change
0.10	0.15	122%
0.15	0.20	74%
0.20	0.25	54%
0.25	0.30	40%
0.30	0.35	32%

From the graph and the table, the effect of the diameter diminishes as it increases. This is because at the certain diameter the flow rate will become practically infinite and increasing the diameter further will not produce significant change.

Both of these graphs indicate that increasing the outlet area increases the Pcrms value and therefore decrease the comfort performance of the cushion. For design purposes however it is important to know how these methods compare with each other. Figure 5.8 shows the results that are obtained when the two were compared. In this case the outlet area is increased from 0.02 in² to 0.08 in². This is done by increasing the

number of outlets from 1 outlet to 4 outlets and in the second case by increasing the outlet diameter from 0.16 inch to 0.32 inch.

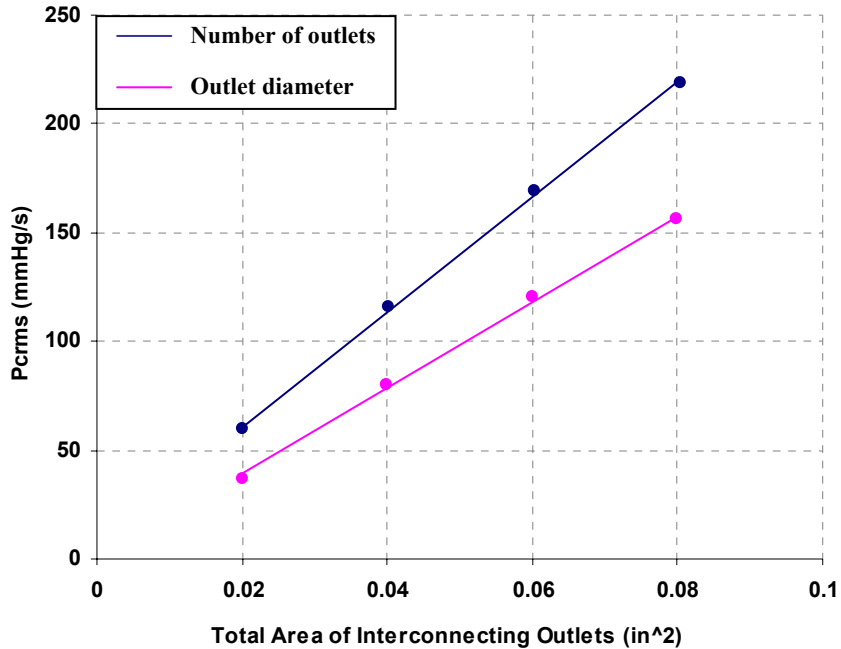


Figure 5.8 A Comparison of how each of the Following; Outlet Number and Outlet Diameter Affect Seat Cushion Comfort Performance in Outlet Area

The graph shows that the seat cushion comfort performance is better when the outlet area is increased by increasing the outlet diameter as opposed to increasing the number of outlets. The fact that the Pc rms value increases as the outlet area increases suggests that to optimize comfort performance it is best to reduce the outlet area to a minimum value. While this may be true in terms of pressure change rate, it is important to note that decreasing the outlet area increases the damping in the cushion and this can reduce the ability of the cushion to isolate vibrations, which can lead to discomfort.

This section concludes the results on the effects that the cushion dimensions have on the comfort performance of an air-inflated cushion. The next section looks at the effect of the material properties that affect the cushion performance.

5.5 Cushion Material Properties

This section examines how material properties affect the comfort performance of the air-inflated seat cushion. Although there are several material properties that can affect driver comfort such as material breathability, our main concern is the factors that will affect pressure related issues. For this reason, the only material property we consider is the elasticity of the material.

5.5.1 Elasticity

Air-inflated seat cushions are commonly made of Neoprene rubber which has a Young's Modulus of 0.8 KPa . In this study, the material elasticity is varied from 0.6 KPa to 1.9 KPa . Figure 5.9 shows the results that are obtained.

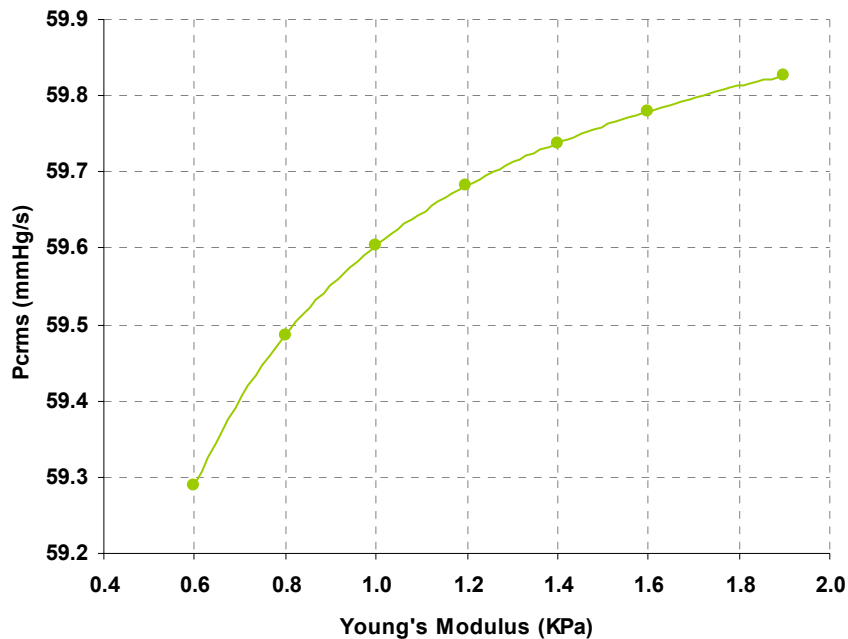


Figure 5.9 Effect of Material Elasticity on the Pc rms Value

Increasing the elastic modulus over this range increases the Pc rms value by 0.91%. While this indicates that the comfort performance of the cushion is lowered by

increasing the elastic modulus, the percentage change is very small as compared to the other changes that have been observed and thus can be considered negligible.

This concludes the work that was done to determine how various cushion parameters affect the comfort performance of an air inflated cushion. The findings so far indicate that:

1. Increasing the seated area increases the comfort performance of an air-inflated seat cushion
2. For optimization purposes it is better to increase the seated area by maintaining the number of cells over which the seated weight is distributed and increase the base radius of each cell
3. Increasing the cell height improves the comfort performance of the cushion but may compromise the pelvis stability of the person sitting on the cushion
4. Increasing the outlet area decreases the comfort performance of the cushion
5. In order not to reduce the vibration isolation ability of the air-inflated cushion, it is necessary to increase the outlet area and the best way to do this is to maintain the number of outlets and increase the outlet diameter
6. Material elasticity does not significantly affect the comfort performance of an air-inflated seat cushion

The next section discusses the study that is done to examine how the seated weight of a person can affect the trends observed above.

5.6 Subject Weight

Based on the validation study done it is clear that as the weight of the driver increases, the Pcrms value will increase. It is of interest to determine how driver weight affects not only the comfort performance of the seat cushion but also the trends that have been observed. To find this out, two studies are done. The first is to keep all the cushion parameters constant and examine how the comfort performance of the cushion is affected

as the weight of the driver is increased. In this study the weight is increased from 110 pounds to 180 pounds. Figure 5.10 show the results that are obtained.

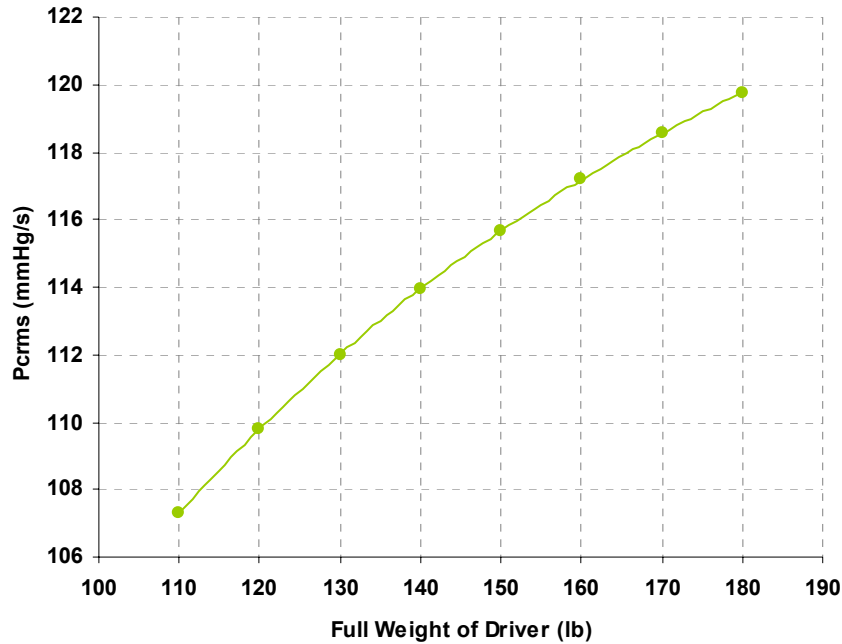


Figure 5.10 Effect of Internal Pressure on the Pc rms Value

As the person's weight is increased the Pc rms value increases indicating a decrease in the comfort performance of the seat cushion. There is a 12% increase in the Pc rms value when a person weighing 180 pounds sits on the cushion as opposed to a person weighing 110 pounds and when compared to the other results that have been seen this is not particularly significant.

5.7 Subject weight Versus Seated Area

The observation made above begs the question as to whether there are significant changes in the trends that have already been observed when different weights are placed on the cushion. To examine these trends each of the above parameters is again examined but this time different weights are applied each time to see what trends emerge.

5.7.1 Subject Weight versus Number of Cells in Seated Area

This section looks at the repeatability of the trends seen previously when the number of cells in the seated area was changed. In this case for every time the cell number is changed, the Pcrms value is recorded for subjects of different weights. The weights used in this study were 180 pounds, 150 pounds and 110 pounds which correspond to a seated weight of 144, 120, 88 pounds respectively. Figure 5.11 shows the results.

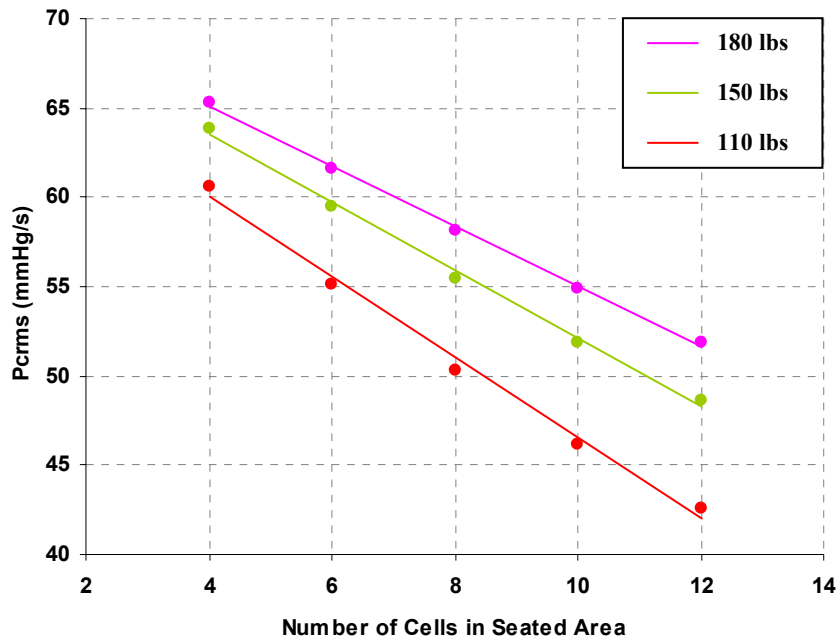


Figure 5.11 A Comparison of the Effects of Different Driver Weights on the Pcrms Value by Varying the Number of Cells in the Seated Area

The trends are similar in that they all show a linear relationship, however they are not parallel to each other indicating that the weight of the driver not only affects the Pcrms value but it affects the slope of the relationship. Table 5.5 shows the percentage decrease in Pcrms value per person over the same change in seated area.

Table 5.6 A Comparison of the Decrease in Pcrms Value per Driver over the Same Change in Cell Number

Weight (lb)	% Decrease in Pcrms Value
110	30%
150	24%
180	21%

Although these changes do not appear to be significant, it indicates that as a person becomes heavier, the ability of the comfort performance of the cushion decreases.

5.7.2 Subject weight Versus Cell Radius

This section examines the repeatability of the trends observed when for a given weight, the cell radius is varied. Figure 5.12 show the results of this study.

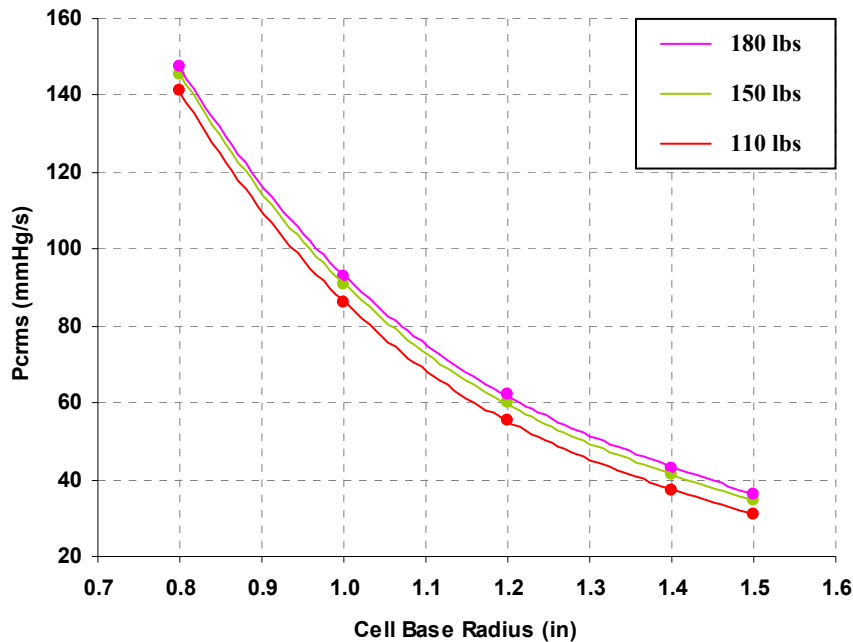


Figure 5.12 A Comparison of the Effects of Different Driver Weights on the Pcrms Value by Varying Seated Area in Terms of the Cell Radius

At a there appears to be no divergence of the graphs away from each other indicating that the weight has no effect on the trend; a closer look shows that although there is at least 30 pounds between each of these weights, there is only a 1% disparity in the percentage

change in the Pcrms value. Table 5.7 shows the percentage drops that were seen per weight in this study.

Table 5.7 A comparison of the Decrease in Pcrms Value per Driver over the Same Change in Cell Radius

Weight (lb)	% Decrease in Pcrms
110	84%
150	83%
180	82%

Although the difference is negligible, the comfort performance of the cushion is better for a lighter person. The next section examines how the trends found in the cell height case change when people of different weights sit on the cushion.

5.8 Subject weight Versus Cell Height

This section examines effect the cell height on the percentage change in the Pcrms value as the driver weight increases. In this case similar to the other cases, the cell height was varied for each driver and the trends examined. Figure 5.13 shows the results.

The results indicate that the weight of the driver has no effect on the Pcrms value when the cell height is being varied. As shown in Table 5.8 each person experiences a 74% reduction in the Pcrms value over the same change in cell height.

Table 5.8 A comparison of the Increase in Pcrms Value per Driver over the Same Change in Cell Height

Weight (lb)	% Increase in Pcrms
110	74%
150	74%
180	74%

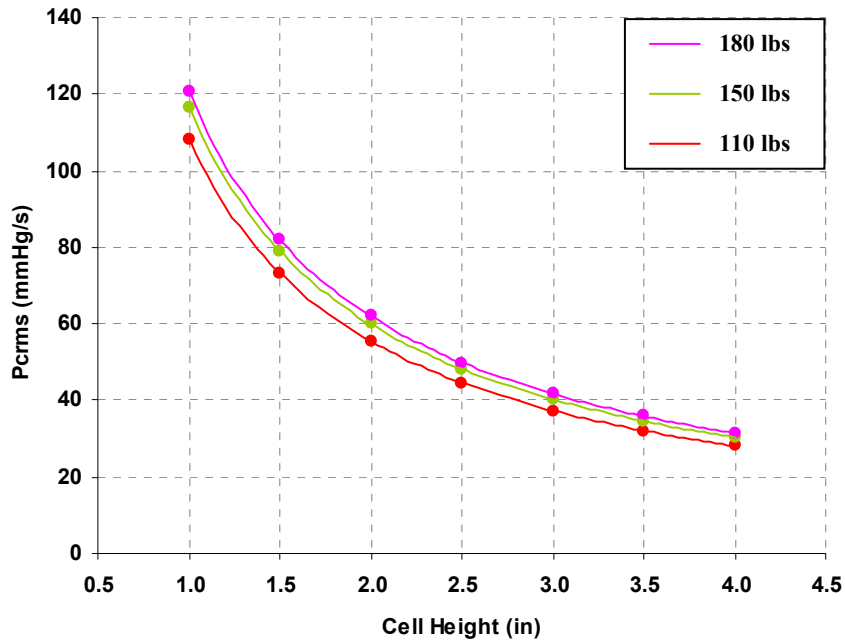


Figure 5.13 A Comparison of the Effects of Different Driver Weights on the Pcrms Value by Varying the Cell Height

The next parameter to be examined in relation to the weight of the driver is the trend seen when the outlet area was varied. The next section discusses the results that were found.

5.9 Subject weight Versus Outlet Area

As mentioned previously, the outlet area provides control over the flow of air from cell to cell. It has been established that as the outlet area increases the Pcrms value increases. What is of interest and needs to be determined is whether people of different weights will experience the same percentage increase in Pcrms value over the same increase in outlet area. This section shows the results that are obtained from examining the effects different subjects would have on the trends observed in section 5.4.

5.9.1 Subject weight Versus Number of Outlets

This section looks at how the Pcrms value is affected by drivers of different weight when the outlet area is being varied. In this case the outlet number is being increased from 0

outlets to 4 outlets while maintaining the diameter of each outlet. Figure 5.14 shows the results obtained. It is not clear from the graph whether there is a difference in the percentage change in the Pcrms value as the driver weight is increased.

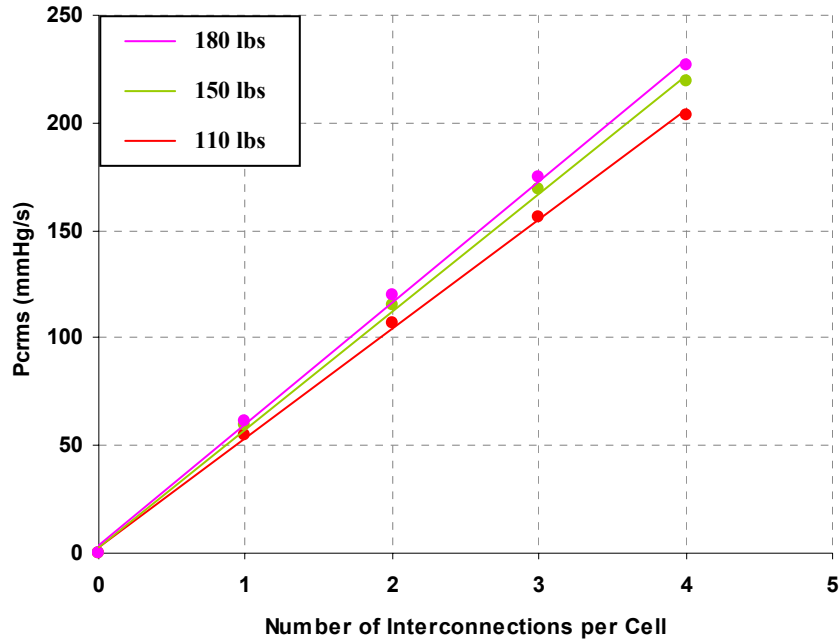


Figure 5.14 A Comparison of the Effects of Different Subject Weights on the Pcrms value by Varying the Number of Outlets per Cell

The data in Table 5.9 however shows that regardless of the driver weight, the percentage change in the Pcrms value remains the same.

Table 5.9 A comparison of the Increase in Pcrms Value per Driver over the Same Change in the Outlet number

Weight (lb)	% Increase in Pcrms
110	268%
150	268%
180	268%

The next case study involves increasing the outlet area but this time it is done by holding the number of outlets constant and increasing the diameter of each outlet by the

same amount. Again in this case the Pcrms value was recorded for drivers of different weights.

5.9.2 Subject weight Versus Outlet Diameter

This section looks at how the Pcrms value is affected by drivers of different weight when the outlet area is being varied. In this case the outlet diameter is being increased from 0 outlets to 0.35 inches while maintaining the number of outlets. Figure 5.15 shows the results obtained. Much like in the previous case it is not clear from the graph whether there is a difference in the percentage change of the Pcrms value as the driver weight is increased.

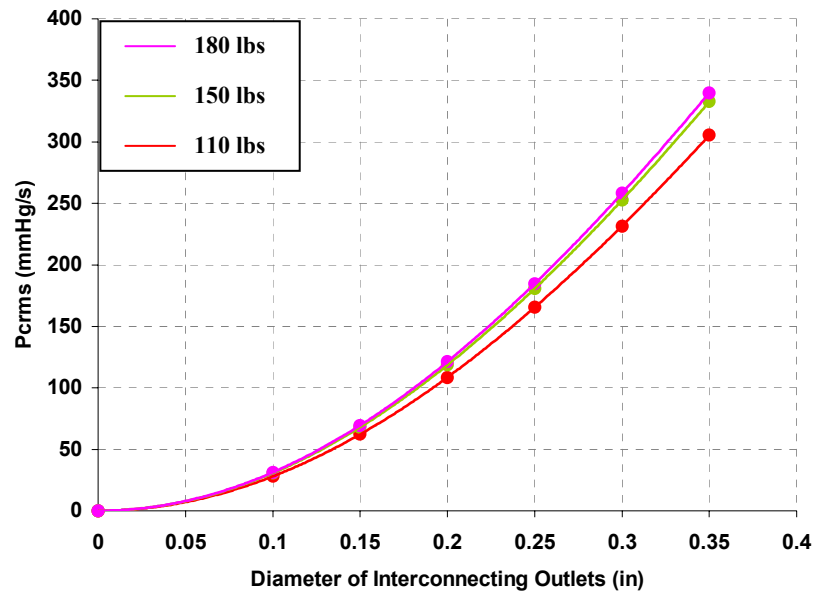


Figure 5.15 A Comparison of the Effects of the Different Subject Weights on the Pcrms value by Varying the Outlet Diameter

An closer look at the data reveals that similar to the method in which the outlet area was increased by increasing the number of outlets, the driver weight does not effect the percentage change in the Pcrms value. Table 5.10 shows the results.

Table 5.10 A comparison of the Increase in Pcrms Value per Driver over the Same Change in Outlet Diameter

Weight (lb)	% Increase in Pcrms
110	389%
150	389%
180	389%

The next section examines how driver weight affects the percentage changes that are seen in the Pcrms value as the elasticity of the material is varied.

5.10 Subject weight Versus Material Elasticity

As the weight of the driver increases, we know that the Pcrms value increases and as such it is expected that for each subject the Pcrms values will increase as the elastic modulus increases. This study determines if the percentage change in Pcrms value is dependent on the weight of the driver when the elasticity of the material is being varied. Figure 5.16 shows the results that are obtained.

The results show that as the weight of the of the driver increases, the percentage change in the Pcrms value increases, over the same change in elastic modulus. This means that as the weight increases although it is a heavier person and therefore there will be a greater expansion in the material, the data indicates that, the expansion is not great enough to accommodate for the increase in weight, and as such the pressure and the pressure change rate increase. Table 5.11 shows the percentage increase in Pcrms value per user over the same change in material elastic properties.

Table 5.11 A comparison of the Overall Decrease in Pcrms Value per Subject over the Same Change in Material Elasticity

Weight (lbs)	% Increase in Pcrms
110	0.61%
150	0.91%
180	1.12%

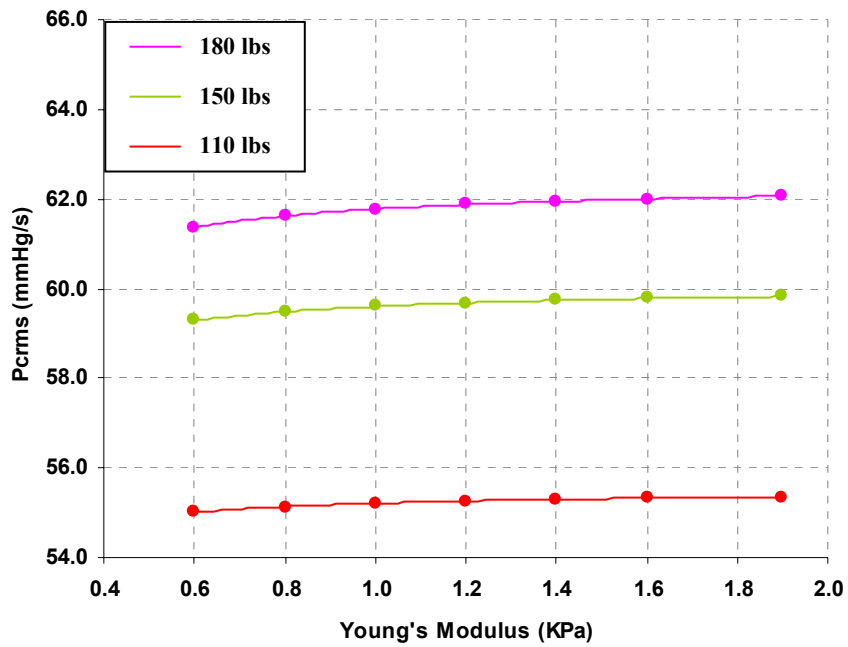


Figure 5.16 A Comparison of the Effects of Different Driver Weights on the Pc rms value by Varying the Material Elasticity

This concludes the results section. The next section concludes and summarizes the work that was done for this thesis and makes recommendations on any further study.

6 Conclusion and Recommendations

This chapter summarizes and concludes the research that was done for this thesis. The objective of the research was to create a mathematical model of an air-inflated seat cushion and to use this model to determine how the comfort performance of an air-inflated seat cushion is affected by modifying various parameters of the cushion. Comfort was determined using a measure of comfort developed by the Daihatsu Motor Company which is dependent on the RMS value of the pressure change rate of the system. The model was developed using MatLab[®] and SimuLINK[®]. After validating the model by varying a number of parameters for which the behavior was known, the model was passed as suitable to be used in this study.

This research examined how the seated area, cell height, outlet area and material stiffness affect the comfort performance of air-inflated cushions. The study went further to examine whether these effects remained the same for drivers of different weights.

The seated area could be modified in two ways, one way was to vary the number of cells over which the drivers seated weight was distributed, while maintaining the cell radius and the other was to maintain the number of cells while varying the radius of each cell. Regardless of which method the following was found:

- The comfort performance of the cushion improved as the seated area was increased.
- Increasing the seated area by increasing the cell radius and holding the number of cells in the seated area constant proved to be a more efficient way to increase comfort performance.
- The comfort performance of the cushion decreased as the driver's weight increased.
- In order to increase the comfort performance of an air-inflated seat cushion for a wide range of weights, it is better to increase that seated area by holding the number of cells constant and increasing the base radius of each cell.

The next aspect of the cushion to be examined was the cell height. The results indicate that:

- Increasing the cell height increased the comfort performance of the cushion but could reduce the pelvic stability of the driver.
- The comfort performance of the cushion is not affected by the weight of the driver when the cell height is varied.

In order to compare cell height with the other parameters that affect the dimensions of each cell, the changes observed were examined in terms of volume. Generally it was found that increasing the seated volume increases the comfort performance of the cushion. In this case increasing the cell radius was still the most effective way to increase comfort performance and increasing the number of cells was the least effective method.

The effect of the outlets on comfort is intuitive, in that the larger the outlets the faster the air will rush from cell to cell and the more uncomfortable it will be. The research done examined which of the two methods of changing the outlet area would produce the best comfort performance. The results show that:

- Increasing the outlet area decreased the comfort performance of the cushion but could increase the ability of the cushion to isolate vibrations.
- Varying the outlet diameter while holding the outlet number gives a better comfort performance than changing the number of outlets.
- The percentage change in the Pcrms value is not affected by the weight of the driver

The final property of the cushion to be examined was the elasticity of the material. The findings indicate that:

- Increasing the material elasticity does not significantly affect the comfort performance of air-inflated seat cushions.
- Although the comfort performance decreases as the weight of the driver increases, the change is negligible.

The above study examined the comfort performance of air-inflated seat cushions as a function of the pressure change rate. The study uses the Pressure Change Root Mean Square Value (Pcrms) to determine how the comfort performance of an air-inflated seat cushion changes as various cushion parameters are varied. Although this study has been able to show how various parameters can affect comfort performance, it is not suggesting that anyone of these parameters is solely responsible for seating comfort. In order to fully optimize the air-inflated cushion, it is necessary for further studies to be done that will look at the effects of all the possible parameter variation combinations to determine how they interact with each other to increase comfort performance. Secondly it is important to determine how varying the parameters examined in this study will affect other factors that can affect comfort performance such as the ability of the cushion to isolate vibrations.

The results in this study do not show an optimal value for any of the parameters that were changed. They simply show what trends can be expected. In order to find what variations will produce optimal comfort performance, it is important to carry out a study that will relate the Pcrms value to actual subjective measures. In other words a Pcrms value or a range of Pcrms values must be identified that can represent what is “comfortable” for a driver.

REFERENCES

1. Gruber, G. J., 1976, "Relationship between Wholebody Vibration and Morbidity Patterns Among Interstate Truck Drivers", Southwest Research Institute, San Antonio, Texas. Center for Disease Control Publication No.77-167, Cincinnati, Ohio.
2. Kiosak, M., 1976, "A Mechanical Resting Surface: it's Effects on Pressure Distribution", *Arch. Phys. Med. Rehabil.* 57, 481-484.
3. Brienza, D. M., Chung, K. C., Brubaker, C. E., Wang, J., Karg, T. E., Lin, C. T., 1996, "A System for the Analysis of Seat Support Surfaces Using the Surface Shape Control and Simultaneous Measurement of Applied Pressure", *IEEE Trans. Rehabil. Eng.* 4, 103-113.
4. Apatsidis, D. P., Solomonidis, S. E., Michael, M. S., 2002, "Pressure Distribution at the Seating Interface of Customer-Molded Wheelchair Seats: Effects of Various Materials", *Arch. Phys. Med. Rehabil.* Vol. 83, 1151-1156.
5. Hostens, I., Papaioannou, G., Spaepen, A. and Ramon, H., 2001, "Buttocks and Back Pressure Distribution Tests on Seats of Mobile Agricultural Machinery", *Applied Ergonomics* 32, 347-355.
6. Huston, D. R., Johnson, C. C., Wood, M. A., Zhao, X., 1998, "Vibration Attenuation Characteristics of Air Filled Seat Cushions", *Journal of Sound and Vibration*, 222(2), 333-340.
7. Goldman, D.E. and VonGierke, H.E., 1960, "The Effect of Shock and Vibration on Man" Naval Medical Research Institute, Lecture and Review Series No. 60-3, Bethesda, Maryland.
8. Buckle, P., Fernandes, A., 1998, "Mattress Evaluation – Assessment of Contact Pressure, Comfort and Discomfort", *Journal of Applied Ergonomics*, 29(1), 35-39.

9. Huston, D. R., Zhao, X., Johnson, C. C., 2000, "Whole-Body Shock and Vibration: Frequency and Amplitude Dependence of Comfort", *Journal of Sound and Vibration* (2000) 230(4), 964-970.
10. Borg, G., 1982, "Psychophysical Judgment and the Process of Perception", Geissler and Petzold, Editors, 25-33. Berlin: VEB Deutscher Verlag der Wissenschaften. "A Category Scale with Ratio Properties for Intermodal and Interindividual Comparisons".
11. Uenishi, K., Fujihashi, K., Imai, H., 2000, "A Seat Ride Evaluation Method for Transient Vibrations", SAE Technical Paper 2001-01-0641.
12. Floyd, W.F., Roberts, D.F., 1958, "Anatomical and Physiological Principles in Chair and Table Design". *Ergonomics* 2, 1-16, Kharagpur, India.
13. Viano, D.C., Andrzejak, D. V., 1992, "Research Issues on the Biomechanics of Seating Discomfort: an Overview with Focus on Issues of the Elderly and Low-Back Pain", Society of Automotive Engineers, Technical Paper Series 920130.
14. Van Niekerka, J. L., Pielemeierb, W.J., Greenberg, J.A., 2003, "The use of Seat Effective Amplitude Transmissibility (SEAT) Values to Predict Dynamic Seat comfort", *Journal of Sound and Vibration* 260, 867–888.
15. Andreoni, G., Santambrogio, G. C., Rabuffetti, M., Pedotti, A., 2002, "Method for the Analysis of Posture and Interface Pressure of Car Drivers", *Journal of Applied Ergonomics*, 33, 511–522.
16. Falou, E. W., Duchêne, J., Grabisch, M., David Hewson, Yves Langeron, Lino, F., 2002, "Evaluation of Driver Discomfort during Long-Duration Car Driving", *Journal of Applied Ergonomics*.
17. Paddan, G. S. and Griffin, M. J., 2002, "Effect of Seating on Exposures to Whole-Body Vibration in Vehicles", *Journal of Sound and Vibration*, 253(1), 215-241.
18. <http://www.openerg.com/seating.htm>

19. Kang, T. E., Mak, A. F., 1981, "Development of a Simple Approach to Modify the Supporting Properties of Seating Foam for Pressure Relief", *J. Rehabil. Res. Dev.*, 35 (Pt 1), 52-60.
20. Porter, J. M., Gyi, D. E., Tait, H. A., 2002, "Interface Pressure Data and the Prediction of Driver Discomfort on Road Trials", *Journal of Applied Ergonomics*.
21. Shen, W., Parsons, C. K., 1997, "Validity and Reliability of Rating Scales for Seated Pressure Discomfort", *International Journal of Ergonomics*, 20, 441-461.
22. Seigler, M., 2002, "A Comparative Analysis of Air-inflated and Foam Seat Cushions for Truck Seats", Virginia Polytechnic Institute and State University, Blacksburg, Virginia.
23. <http://www.rohoinc.com/commercial/ahtruck.jsp>
24. Ashby, M.F., Cebon, D., 2002, "Unit 1. Mapping the World of Materials: the First Step in Exploration and Selection", *New Approaches to Materials Education*, Cambridge, UK.

APPENDIX A

clear all;

close all;

```
%~~~~~ DRIVER PROPERTIES AND INPUTS ~~~~~  
Weight = 110;           % weight of driver in pounds  
W = 0.8*Weight;        % upper body weight of driver in pounds
```

```
%~~~~~ CONSTANTS ~~~~~  
g = 384;                % acceleration due to gravity in feet per second squared  
pi = 3.141;            % pi  
R = 18540;              % ideal gas constant
```

```
%~~~~~ CUSHION PROPERTIES ~~~~~  
r = 1.2;                % base radius of bubble in inches  
h = 2;                  % height of bubble in inches  
P_bar = 0.77355;        % gauge pressure in bubble in pounds per square inch  
D = 0.16;               % orifice diameter in inches  
l = 0.43;               % orifice length in inches  
V_init = 2/3*pi*r^2*h;  
A_init = pi*r^2;
```

```
%~~~~~ FLOW CALCULATIONS ~~~~~  
Re_D = ((0.8*1)/D)/0.05; % Reynolds number  
n = 4;                  % number of orifices  
if n <= 0;  
    n = 0;  
elseif n > 4;  
    n = 4;  
end  
N = 6;                  % number of bubbles  
N_max = 12;  
if N <= 4;  
    N = 4;  
elseif N > N_max;  
    N = N_max;  
end
```

```
Neoprene = 0.8e-3*10e9; % modulus of elasticity for rubber in  
E = Neoprene * 1.450377e-4; % modulus of elasticity for rubber in
```

```
if n <= 0;  
    D = 0;  
elseif n > 0;
```

```

    D = D;
end

%~~~~~ AIR PROPERTIES ~~~~~
rho = 1e-2;           % density of air in slug per feet cubed
P_atm = 14.696;      % atmospheric pressure
T = 580.67;         % temperature of air (77F 25C)
MM_air = 0.06384;   % molar mass of air
P = rho*R*T;
m = V_init*rho;

%~~~~~ SIMULATE SATURATIONS ~~~~~
sim ('in_the_beginning')

%~~~~~ INITIAL CONDITIONS ~~~~~
deltaV = deltaV;
mean_deltaV = mean(deltaV);
mean_deltaV1 = -mean(deltaV);

%~~~~~ SIMULATE STATIC CONDITIONS ~~~~~
sim ('ha')

%~~~~~ PLOTS ~~~~~
y = P_one;
dy = dP_one

figure
disp(P1vsTime([1:2],:));
subplot(2,2,1);
plot (P1vsTime(:,1),P1vsTime(:,2));
title('Pressure Change in Seated Area');
ylabel('Pressure (mmHg)');
grid on;

disp(P1dtvsTime([1:2],:));
subplot(2,2,2);
plot (P1dtvsTime(:,1),P1dtvsTime(:,2));
axis([0 2 -150 0]);
title('Rate of Pressure Change in Seated Area');
ylabel('dP/dt (mmHg/s)');
grid on;

disp(P2vsTime([1:2],:));
subplot(2,2,3);
plot (P2vsTime(:,1),P2vsTime(:,2));
title('Pressure Change in Non-Seated Area');

```

```
ylabel('Pressure (mmHg)');  
grid on;
```

```
disp(P2dtvsTime([1:2],:));  
subplot(2,2,4);  
plot (P2dtvsTime(:,1),P2dtvsTime(:,2));  
axis([0 2 0 150]);  
title('Rate of Pressure Change in Non-Seated Area');  
ylabel('dP/dt (mmHg/s)');  
grid on;
```

VITA

Name: Akua Boabema Ofori-Boateng

Place and Year of Birth: Accra, Ghana, 1976

Education: Virginia Polytechnic Institute and State University, Blacksburg, Virginia, Master of Science in Mechanical Engineering, 2001-2003.

Miami University, Oxford, Ohio, Bachelor of Science in Engineering Physics, 1996-1999.

Work Experience: **Actuator Product Engineer**, Cummins Engine Company, Columbus, Indiana, 2003

Graduate Teaching Assistant, Mechanical Engineering Department, Virginia Polytechnic Institute and State University, Blacksburg, Virginia, 2001-2003

Mechanical Engineering Intern, Vodi Technik Motors Ltd., Accra, Ghana, 2002

Research Associate, The Procter and Gamble Company, Cincinnati, Ohio, 2000-2001

Publications: Novel Process for Producing Cubic Liquid Crystalline Nanoparticles (Cubosomes). *Langmuir*, 2001, 17(19), 5748-5756.

Enhanced loading of Water Soluble Actives into Bicontinuous Cubic Phase Liquid Crystals using Cationic Surfactants, *Journal of Colloidal and Interface Science*, 2003, 260, 404-413.